Combinatorial transcriptional control of the lactose operon of *Escherichia coli*

Thomas Kuhlman*, Zhongge Zhang†, Milton H. Saier, Jr.†, and Terence Hwa*‡

*Center for Theoretical Biological Physics and †Division of Biological Sciences, University of California at San Diego, La Jolla, CA 92093-0374

Edited by Carol A. Gross, University of California, San Francisco, CA, and approved January 29, 2007 (received for review August 7, 2006)

The goal of systems biology is to understand the behavior of the whole in terms of knowledge of the parts. This is hard to achieve in many cases due to the difficulty of characterizing the many constituents involved in a biological system and their complex web of interactions. The *lac* promoter of *Escherichia coli* offers the possibility of confronting "system-level" properties of transcriptional regulation with the known biochemistry of the molecular constituents and their mutual interactions. Such confrontations can reveal previously unknown constituents and interactions, as well as offer insight into how the components work together as a whole. Here we study the combinatorial control of the *lac* promoter by the regulators Lac repressor (LacR) and cAMP-receptor protein (CRP). A previous *in vivo* study [Setty Y, Mayo AE, Surette MG, Alon U (2003) *Proc Natl Acad Sci USA* 100:7702–7707] found gross disagreement between the observed promoter activities and the expected behavior based on the known molecular mechanisms. We repeated the study by identifying and removing several extraneous factors that significantly modulated the expression of the *lac* promoter. Through quantitative, systematic characterization of promoter activity for a number of key mutants and guided by the thermodynamic model of transcriptional regulation, we were able to account for the combinatorial control of the *lac* promoter quantitatively, in terms of a cooperative interaction between CRP and LacR-mediated DNA looping. Specifically, our analysis indicates that the sensitivity of the inducer response results from LacR-mediated DNA looping, which is significantly enhanced by CRP.

DNA looping | gene regulation | *lac* promoter | systems biology

The *lac* promoter (P*lac*) of *Escherichia coli* is one of the most extensively studied systems of molecular biology (1–6). The knowledge and insight gained from these studies have shaped much of how we now think about gene regulation. It is well known that *E. coli* cells repress the expression of the *lac* operon when glucose is abundant in the growth medium. Only when the glucose level is low and the lactose level is high is the operon fully expressed. Thus, the regulation of this operon represents an example of "combinatorial control" widely seen in prokaryotes and eukaryotes (7, 8). In this case, the combinatorial control is implemented molecularly by two transcription factors, the Lac repressor (LacR), which represses transcription and the cAMP receptor protein (CRP) which activates transcription. Activation by CRP requires the inducer cAMP, which is used by *E. coli* cells as a signal of glucose shortage (9–15). Repression by LacR is activated in a nearly all-or-none manner upon varying the amount of lactose or one of the several synthetic inducers in growth medium with poor carbon sources (16, 17). The fold-change in repression is very large (>1,000-fold) and has been shown to involve LacR-mediated DNA looping (5, 6, 18–21).

Here we quantitatively investigate the competing effects of activation and repression on the P*lac in vivo*. We focus on two perplexing issues. (*i*) According to biochemical studies (22–25), LacR–inducer interaction is only weakly cooperative. By what mechanism(s) does the observed induction response become so abrupt (26, 27)? (*ii*) Despite the well known role CRP plays in activating transcription (28), structural studies (29, 30) suggest that CRP enhances repression by facilitating the LacR-mediated DNA looping. Moreover, *in vitro* biochemical studies indicate that CRP stabilizes LacR–DNA binding (31–33). What functional role(s) does CRP actually play in the control of this operon? We approached these issues by first identifying mutants of *E. coli* MG1655 that allowed us to directly control the activities of the activators and repressors by varying the levels of two inducers in the growth medium. We then characterized the promoter activity systematically for numerous combinations of the inducers. The gene expression data obtained clearly reveal the effect of CRP in enhancing the steepness of the inducer response. We developed a thermodynamic model of gene regulation (8, 34–36), incorporating the known molecular mechanisms of LacR-induced DNA looping and its coupling to CRP through DNA bending (32, 33). The success of the model is manifested in its ability to describe the complex codependence of gene expression on the two inducer levels quantitatively by invoking a single parameter, the cooperativity between CRP and LacR-mediated DNA looping, with the fitted value of the cooperativity agreeing well with that determined from *in vitro* biochemical measurements (32, 33). Our study presents a proof of concept that the complicated web of interactions that couple repressors, activators, promoters, and DNA loops *in vivo* can be quantitatively dissected, provided that the right modeling together with a precise sequence of experiments on a systematically picked set of mutants are carried out.

Results

Repression by LacR. We first quantitatively characterized the activity of the P*lac* subject to various degrees of repression by the LacR for *E. coli* cells in the exponential growth phase. In our experiments, the activity of LacR was modulated by the synthetic gratuitous inducer isopropyl β-D-thiogalactopyranoside (IPTG) (37). We performed the β-galactosidase assays for wild-type *E. coli* MG1655 cells in M9 minimal medium with 0.5% glucose as the carbon source and up to 1 mM IPTG. P*lac* activity, defined here as the product of the β-galactosidase activity and the cell-doubling rate [see supporting information (SI) *Methods*], is plotted against the corresponding IPTG concentrations as the black crosses in Fig. 1*a*.

The data points are fitted to the Hill function,

$$\alpha_{\mathrm{IPTG}} = b_{\mathrm{IPTG}} \cdot \frac{1 + f_{\mathrm{IPTG}} \cdot ([\mathrm{IPTG}]/C_{\mathrm{IPTG}})^{m_{\mathrm{IPTG}}}}{1 + ([\mathrm{IPTG}]/C_{\mathrm{IPTG}})^{m_{\mathrm{IPTG}}}}, \qquad [1]$$

Author contributions: M.H.S. and T.H. designed research; T.K. and Z.Z. performed research; T.K. analyzed data; T.K. and T.H. wrote the paper; and M.H.S. provided training and references.

The authors declare no conflict of interest.

This article is a PNAS Direct Submission.

Abbreviations: LacR, Lac repressor; CRP, cAMP-receptor protein; IPTG, isopropyl β-D-thiogalactopyranoside; AC, adenylate cyclase; PDE, cAMP-phosphodiesterase.

‡To whom correspondence should be addressed at: Center for Theoretical Biological Physics, University of California at San Diego, 9500 Gilman Drive, La Jolla, CA 92093-0374. E-mail: hwa@ucsd.edu.

This article contains supporting information online at www.pnas.org/cgi/content/full/0606717104/DC1.

© 2007 by The National Academy of Sciences of the USA

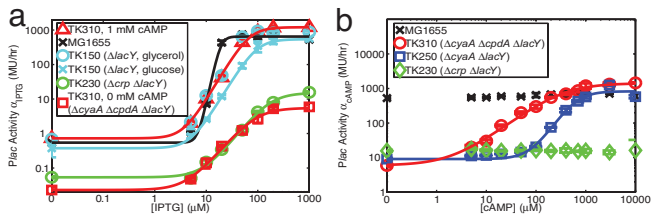

Fig. 1. Dependence of P*lac* activity on the inducers. (*a*) The IPTG response for *E. coli* MG1655 and various Δ*lacY* mutants grown in minimal M9 medium with various amounts of IPTG and 0.5% glucose except for the cyan circles (0.5% glycerol). No cAMP was added to the medium except for the red triangles, which indicate that 1 mM cAMP was added. The lines are best fits to the Hill function (Eq. **1**). (*b*) The cAMP response for *E. coli* MG1655 and various Δ*cyaA* mutants, grown in minimal M9 medium plus 0.5% glucose, 1 mM IPTG, and various amount of cAMP. The lines are best fits to the Hill function (Eq. **2**).

shown as the black line in Fig. 1*a*. The Hill function is used here (and elsewhere in *Results*) merely to extract the qualitative features of the promoter activity; the appropriate quantitative description of the data presented will be provided below in *Analysis*. The features of the IPTG-dependent promoter activity (the "IPTG response") are conveyed by the best-fit Hill parameters listed in Table 1 (row 1): The overall fold change, quantified by $f_{\mathrm{IPTG}} \approx 1{,}200$, is in good agreement with previous studies (5, 6, 18–20, 38, 39). However, the "sensitivity" of the response, quantified by the slope of the transition region in a log–log plot and given approximately by the Hill coefficient ($m_{\mathrm{IPTG}} \approx 4.5$), is much larger than the expected behavior based on the known biochemistry (see below).

One factor contributing to the hypersensitivity observed is a positive-feedback effect due to the expression of *lacY*, which encodes the Lac permease, as previously reported (16, 39). We therefore deleted *lacY* from *E. coli* MG1655 to form strain TK150 (see SI Table 4), and repeated the β-galactosidase assays for this strain. P*lac* activities obtained are plotted as the cyan crosses in Fig. 1*a*. Fitting again to the Hill form yields the cyan line with the best-fit parameters shown in Table 1 (row 2). The IPTG response of the Δ*lacY* mutant exhibits a broader transition, with $m_{\mathrm{IPTG}} \approx 2.6$.

Another possible cause of this hypersensitivity is a suggested cooperative interaction between the LacR and the activator CRP, which also binds in the promoter region (31–33). To investigate this possibility, we deleted the *crp* gene from *E. coli* TK150 to form strain TK230 (SI Table 4) and repeated the β-galactosidase assays for this strain. P*lac* activities obtained are plotted as the green circles in Fig. 1*a*. Fitting again to the Hill form yields the green line with the best-fit parameters shown in Table 1 (row 3). The IPTG response of the Δ*crp* Δ*lacY* double mutant is broader still, with $m_{\mathrm{IPTG}} \approx 2$.

Activation by CRP. We next characterized the dependence of P*lac* activity to different degrees of activation by cAMP–CRP (the "cAMP response"). To avoid possible complications due to interaction between LacR and CRP, all experiments were performed under saturating IPTG concentration (1 mM) to disable LacR–operator interaction. This was complemented by direct deletion of LacR in some cases (see below). We also deleted *lacY* in all subsequent experiments to avoid possible feedback. In all cases discussed below where we directly compared the P*lac* activity of *lacY* $^-$ and *lacY*$^+$ cells, differences of no more than 2-fold were obtained (data not shown).

Table 1. Hill parameters for the IPTG response

Strain	b_{IPTG}, MU/hr	f_{IPTG}	C_{IPTG}, μM	m_{IPTG}
MG1655	0.5	1,200 ± 80	20 ± 4	4.5 ± 0.7
TK150 (Δ*lacY*)	0.4	1,445 ± 185	100 ± 18	2.6 ± 0.2
TK230 (Δ*crp* Δ*lacY*)	0.05	255 ± 19	150 ± 15	2.0 ± 0.1
TK310 (Δ*cyaA* Δ*cpdA* Δ*lacY*), no cAMP	0.02	238 ± 26	90 ± 5	2.0 ± 0.2
TK310, 1 mM cAMP	0.7	1,600 ± 180	70 ± 8	2.8 ± 0.1

Parameters derived from fit of the IPTG dependence of the P*lac* activity to the Hill form (Eq. **1**) for various strains of *E. coli* derived from MG1655, grown in medium with 0.5% glucose and various amounts of IPTG. For the last row, 1 mM cAMP was also added to the growth medium. MU, Miller unit.

Control by cAMP. One way to manipulate the cellular level of cAMP–CRP is to subject cells to different levels of cAMP in the medium and rely on the diffusion of cAMP into cells. This approach requires shutting off the endogenous synthesis of cAMP by the enzyme adenylate cyclase (AC), encoded by *cyaA* (41–44). Setty *et al.* (28) attempted this approach by growing cells in medium with 0.2% glucose and various levels of cAMP, expecting that AC activity would be repressed via catabolite repression (10, 14, 15, 45–49). However, they observed only a few-fold change in P*lac* activity despite large variations in the extracellular cAMP levels (0–20 mM) (27). The observed change was surprisingly small given that >50-fold difference in P*lac* activity was obtained between the wild-type and Δ*crp* strains (3). In fact, a nearly 10-fold difference in P*lac* activity can be seen by simply growing wild-type cells on various sugars [see SI Fig. 3 (blue bars)].

Effect of AC deletion. We reasoned that the small change in P*lac* activity obtained by Setty *et al.* (28) might have resulted from the incomplete repression of AC activity by glucose uptake; hence, we repeated the experiment with the deletion of *cyaA*. *E. coli* TK250 strain (Δ*cyaA* Δ*lacY*; see SI Table 4) was grown in M9 minimal medium with 0.5% glucose, 1 mM IPTG, and up to 10 mM cAMP. β-Galactosidase activity was assayed as described above. The resulting P*lac* activity displays a smooth sigmoidal dependence as shown in Fig. 1*b* (blue squares). [Almost identical results (data not shown) were obtained for the *LacR*-null mutant (strain TK320), indicating that LacR is indeed not a factor with saturating IPTG (1 mM) in the growth medium.] A ≈100-fold difference is seen between the low and high cAMP concentrations, comparable to the difference in P*lac* activity reported between the *crp*-null mutant and wild-type strains of *E. coli* (3). In contrast, P*lac* activity of the wild type (Fig. 1*b*, black symbols) as well as the Δ*lacY* mutant (data not shown) grown in glucose displayed only an ≈3-fold change over the same range of cAMP levels, similar to the before-mentioned finding by Setty *et al.* (28). As a negative control, we show in Fig. 1*b* (green circles) the promoter activity obtained for the *crp*$^-$ strain (TK230); its lack of cAMP dependence indicates that the observed cAMP dependence for the *crp*$^+$ strain was mediated primarily by cAMP–CRP. Additional negative controls on possible indirect effects of cAMP variations on P*lac* activity are shown in SI Fig. 4*b*. We found the variation of CRP expression and the nonspecific effects of CRP on P*lac* activity to be small (≈2-fold), compared with the 100-fold difference observed for the Δ*cyaA* mutants over the same range of cAMP concentrations.

The cAMP response exhibited by strain TK250 was analyzed by fitting to the Hill function,

$$\alpha_{\mathrm{cAMP}} = b_0 \cdot \frac{1 + f_{\mathrm{cAMP}} \cdot ([\mathrm{cAMP}]/C_{\mathrm{cAMP}})^{m_{\mathrm{cAMP}}}}{1 + ([\mathrm{cAMP}]/C_{\mathrm{cAMP}})^{m_{\mathrm{cAMP}}}}, \qquad [2]$$

and plotted as the blue line in Fig. 1*b*. The best-fit parameters are shown in Table 2 (row 1). The sensitivity of the cAMP response, characterized by the Hill coefficient $m_{\mathrm{cAMP}} \approx 2$, is in disagreement with the noncooperative nature of cAMP–CRP interaction (50–53). This suggests a nonlinear relationship between the extracellular and intracellular cAMP concentrations in Δ*cyaA* strain and prompted us to look for additional factors regulating intracellular cAMP levels.

Effect of phosphodiesterase deletion. One such factor is cAMP degradation catalyzed by the enzyme cAMP-phosphodiesterase (PDE) (54–58), encoded by *cpdA* (59). We deleted the *cpdA* gene to obtain

Table 2. Hill parameters for the cAMP response

Strain	b_{cAMP}, MU/hr	f_{cAMP}	C_{cAMP}, μM	m_{cAMP}
TK250 (Δ*cyaA* Δ*lacY*)	9.1	91 ± 5	645 ± 43	2.1 ± 0.1
TK310(Δ*cyaA* Δ*cpdA* Δ*lacY*)	5.9	240 ± 13	320 ± 32	1.0 ± 0.1
Prediction based on thermodynamics	—	>20	10–1,000	1

The first two rows give the parameters derived from fit of cAMP response of *cyaA* mutants to the Hill function (Eq. **2**). The last row gives the best estimates of these parameters according to the thermodynamic model and the known biochemical parameters (see *SI Methods* for details).

strain TK310 (Δ*cyaA* Δ*lacY* Δ*cpdA*) (see SI Table 4) and repeated the β-galactosidase assay and analysis. The cAMP response obtained (Fig. 1*b*, red circles) is more gradual than that of *cpdA*$^+$ cells (blue squares). Fitting the data to the Hill form (Eq. **2**) yielded the red line with the Hill parameters listed in Table 2 (row 2). Specifically, the Hill coefficient $m_{cAMP} \approx 1$ is consistent with the naïve expectation based on the noncooperative nature of cAMP–CRP interaction (50–53).

Combinatorial Control. We next investigated the codependence of P*lac* activity on the two regulators, LacR and cAMP–CRP. We showed above that the Δ*crp* Δ*lacY* strain (TK230) could be used to characterize the bare IPTG response, whereas the Δ*lacY* Δ*cyaA* Δ*cpdA* strain (TK310) could be used to characterize the bare cAMP response. To characterize the codependence of the promoter on IPTG and cAMP, we first verified that strain TK310 exhibited nearly the same IPTG dependence as TK230 in growth medium with no cAMP added; compare[§] the red squares and green circles in Fig. 1*a*. Fitting the IPTG response of TK310 (red squares) to the Hill form (Eq. **1**) yields the solid red line; the corresponding parameters are provided in Table 1 (row 4).

We repeated the β-galactosidase assay and analysis for TK310 cells grown in media with various combinations of IPTG and cAMP concentrations. As evidence of an interaction between IPTG-mediated and cAMP-mediated regulations, we show in Fig. 1*a* (red triangles) the IPTG response for TK310 strain in growth medium containing 1 mM cAMP. This response is nearly indistinguishable from the physiological P*lac* activity exhibited by *cyaA*$^+$ *cpdA*$^+$ cells in glycerol medium (cyan circles). The dashed red line is the best fit to the Hill function (Eq. **1**), with parameters listed in Table 1 (row 5). Note that the overall fold-change (f_{IPTG}) is increased from <250-fold when no cAMP was added in the medium to >1,500-fold with 1 mM cAMP in the medium. The latter fold-change is comparable to those obtained for wild-type *E. coli* cells grown in the absence or saturating concentration of IPTG (Fig. 1*a*, black crosses) (5, 6, 18–20, 38, 39). Additionally, the sensitivity of the IPTG response increased from $m_{IPTG} \approx 2.0$ (Table 1, row 4) for TK310 cells grown in the absence of cAMP to $m_{IPTG} \approx 2.8$ (Table 1, row 5) for the same cells grown in 1 mM cAMP. Fitting the IPTG responses of these cells obtained at a variety of cAMP concentrations, we found a trend of increasing Hill coefficient (from 2 to 3) and fold-change (from 250- to 1,800-fold) for cAMP levels from 1 μM to 1 mM (see SI Fig. 5*a*). The complete codependence of P*lac* activity on IPTG and cAMP is shown as the 3D plot in SI Fig. 6*a*.

Analysis

We have seen that the IPTG and cAMP responses of various mutant strains of *E. coli* MG1655 fitted well to Hill functions, with the Hill parameters summarized in Tables 1 and 2. However, the Hill function itself has been invoked so far without justification; it was merely a familiar form used to quantify key features of the response, e.g., the overall fold-change and sensitivity. Below we will analyze and interpret the results obtained in light of the rich knowledge on the molecular biology of the P*lac* and the biochemistry of the associated components using a thermodynamic model of transcriptional regulation (see refs. 8 and 36; see also the brief review in *SI Methods*).

Activation by cAMP–CRP Is Noncooperative. The cAMP response found for strain TK310 (Δ*cyaA* Δ*cpdA* Δ*lacY*) exhibited a broad transition (Fig. 1*b*, red circles), well fitted by the Hill form (red line). This is in agreement with the thermodynamic model, which predicts the Hill form for response to simple activation by cAMP–CRP (*SI Methods*) (35). The Hill coefficient $m_{cAMP} \approx 1$ obtained is in good agreement with the biochemistry finding that it takes one cAMP molecule to activate the CRP dimer (51–53).

The thermodynamic model further relates the other Hill parameters f_{cAMP} and C_{cAMP} to the biochemical parameters that describe CRP-mediated transcriptional activation (see *SI Methods*). The best estimates of f_{cAMP} and C_{cAMP} based on knowledge of the biochemical parameters are given in Table 2 (row 3). The available information is not sufficient for a quantitative comparison of the parameter C_{cAMP}, whose value depends on the CRP–operator binding affinity *in vivo* as well as the relationship between the intra- and extracellular cAMP concentrations, both of which can be estimated only very crudely (*SI Methods*) (9, 60). The parameter f_{cAMP}, which describes the maximal fold-change in the cAMP response, is given by the cooperativity of CRP and RNA polymerase interaction according to the thermodynamic model. Our result $f_{cAMP} = 240 \pm 13$ is significantly larger than the cooperativity factor of ≈20 obtained from *in vitro* biochemical measurements (61, 62). This discrepancy is analogous to one noted earlier by Beckwith *et al.* (3). It may have resulted from the accumulation of a number of small factors. For example, in addition to recruiting RNA polymerase, CRP was shown to stimulate the transition of promoter DNA from the closed to open conformation, thereby enhancing the transcription rate by ≈50% (61). In addition, the autoregulation of CRP expression may account for ≈2-fold difference (see SI Fig. 3), and another ≈2- to 3-fold difference may be attributed to the deletion of *cpdA* (Fig. 1*b*, compare the vertical ranges of the blue and red lines).

PDE Provides Insulation to Variations in cAMP. We are not aware of any significant phenotype reported for cells with a PDE deletion. Only small differences of 2- to 3-fold in P*lac* activity were seen between the wild-type and Δ*cpdA* strains (SI Fig. 3, blue and red bars), and no systematic trend can be seen in the growth rates of the two strains (SI Fig. 3, numbers on top of the bars). However, the effect of *cpdA* expression on the *cyaA* mutant is striking. Comparison of the blue and red lines in Fig. 1*b* suggests that PDE expression insulates the cell from extracellular cAMP variations of up to 100 μM. This may be important for cells in environments where AC activity is significantly repressed.

LacR-Mediated DNA Looping Increases the Sensitivity of the IPTG Response. The IPTG response of the Δ*crp* Δ*lacY* double mutant (TK230) exhibited a reduced sensitivity (Fig. 1*a*, green circles) compared with the *lacY* mutant (TK150; Fig. 1*a*, cyan crosses). The difference is due to the activated CRP in the latter strain (which has *cyaA* intact and, hence, synthesizes cAMP endogenously). We will discuss the effect of CRP shortly; for now, we first discuss the IPTG response in the absence of CRP, i.e., that of strain TK230. This response is well fitted by the Hill form (Fig. 1*a*, green line), with the Hill coefficient $m_{IPTG} \approx 2.0$ (Table 1, row 3). Although a cooperative IPTG response with Hill coefficient ≈ 2 is widely quoted in the molecular biology literature (26) and, moreover, a cooperative IPTG–LacR interaction was suggested based on a structural study of LacR (29), *in vitro* biochemical studies of IPTG–LacR binding

[§]However, *cpdA* mutants show a 2-fold overall reduction in gene expression for unknown reasons.

Table 3. Parameters for model with DNA Looping.

Strain	K_{IPTG}, μM	L_0
TK230 (Δ*crp* Δ*lacY*)	15.7 ± 1.5	4.1
TK310 (Δ*cyaA* Δ*cpdA* Δ*lacY*)	12.3 ± 1.4	3.7
TK250 (Δ*cyaA* Δ*lacY*)	17.8 ± 1.7	5.0

Parameters derived from the fit of IPTG response of given strains to the thermodynamic model with DNA looping (Eq. **3**).

in fact found a noncooperative IPTG–LacR interaction, which became only weakly cooperative (Hill coefficient = 1.4~1.6) in the presence of operator DNA fragments (22–25). We reasoned that the apparent cooperativity ($m_{IPTG} \approx 2$) observed *in vivo* might have resulted from LacR-mediated DNA looping[¶] known to occur in wild-type *E. coli* cells (6, 18–20). The corresponding thermodynamic model is developed in *SI Methods*, with the following form of the IPTG response:

$$\alpha_{IPTG} = \alpha_0 \Big/ \left[1 + \frac{R}{(1 + [IPTG]/K_{IPTG})^2} + \frac{R \cdot L_0}{(1 + [IPTG]/K_{IPTG})^4} \right]. \quad [3]$$

Although Eq. **3** is not of the Hill form, it resembles a spectrum of different Hill functions, with the maximal fold-change

$$f_{IPTG} = 1 + R \cdot (L_0 + 1), \quad [4]$$

and with the sensitivity also increasing with the parameters R and L_0 (see *SI Methods*). The parameter R depends on the LacR concentration and LacR–operator affinity; it gives the fold-repression between zero and saturating IPTG levels in the absence of DNA looping ($L_0 = 0$). The values of $R \approx 20$–50 can be inferred from two previous studies by Oehler *et al.* (6, 21), who characterized the activities of P*lac*s bearing various Lac operator mutations (see *SI Methods*). In the analysis below, we use $R \approx 50$; results of similar quality (data not shown) can be obtained for $R \approx 20$. The parameter L_0 describes the enhancement in the "local concentration" of LacR molecules due to DNA looping (6, 35). There is currently no direct measurement of L_0 for the P*lac* in the absence of CRP binding.

Before applying Eq. **3** to our results, we first discuss its form in the absence of DNA looping ($L_0 = 0$). In a very recent report, Oehler *et al.* (62) used various mutants to characterize the IPTG responses of the P*lac* incapable of DNA looping. Their data are reproduced in SI Fig. 7*a* (red triangles and blue squares) and shown to fit well to Eq. **3** with $L_0 = 0$ (solid line). The data are equally well fitted in SI Fig. 7*b* by the Hill form (Eq. **1**) with an effective Hill coefficient of 1.5, in agreement with results of previous *in vitro* studies (24).

We next confront DNA looping by fitting the IPTG response of strain TK230 (Fig. 1*a*, green circles) to Eq. **3**, with two fitting parameters K_{IPTG} and L_0. (The saturation value α_0 is fixed by the promoter activity at 1 mM IPTG.) The best-fit curve (data not shown) is nearly indistinguishable from the green line in Fig. 1*a*, although Eq. **3** contains one fewer fitting parameter than Eq. **1**. In particular, the observed sensitivity of the IPTG dependence is well reproduced. The best-fit parameters obtained are shown in Table 3 (row 1). The value of the loop parameter simply reflects the maximal fold-change of the IPTG response as given by Eq. **4**. The value of the IPTG–LacR dissociation constant K_{IPTG} obtained is comparable to the results of *in vitro* biochemical studies (*SI Methods*) (4, 64, 65). Similarly, we found that the DNA looping model described the IPTG response of strain TK310 (Δ*cyaA* Δ*cpdA* Δ*lacY*) very well in medium with no cAMP. The corresponding best-fit parameters are given in Table 3 (row 2); the best-fit curve (data not shown) is nearly indistinguishable from the lower red line in Fig. 1*a*.

Cooperativity Between CRP and LacR-Mediated DNA Looping Enhances the Sensitivity of the IPTG Response. Strain TK310, which exhibited the expected cAMP response in medium with 1 mM IPTG and the expected IPTG response in medium with no cAMP added, was used to investigate the combinatorial control of P*lac* activity by LacR and cAMP–CRP. According to the thermodynamic model, if there is no interaction between cAMP–CRP-mediated activation and LacR-mediated repression, then the codependence of P*lac* activity on IPTG and cAMP would simply be the algebraic product of the IPTG response and the cAMP response, i.e., the product of the red lines in Fig. 1. A manifestation of this product form is a simple vertical shift of the IPTG responses of the same strain at different cAMP concentrations in the log–log plots. However, this clearly cannot be the case for strain TK310, because both the sensitivity and the maximal fold-change of its IPTG response increase with increasing cAMP levels (Fig. 1*a* and SI Fig. 5; see also SI Fig. 8*a* for a direct comparison).

Various forms of interactions between CRP and LacR in the P*lac* region have been previously proposed or reported (29, 31–33, 66, 67). Because CRP causes a 90–130° bend in DNA (20, 68, 69), the binding of CRP to its site in the P*lac* could potentially bring the Lac operators O1 and O3 into closer proximity, promoting the formation of DNA loop between them (SI Fig. 9) (29). The existence of this interaction is supported by a computational study based on the available LacR–operator and CRP–operator cocrystal structures (30). Moreover, Hudson and Fried (33) and Vossen *et al.* (34) found cooperativity in the formation of a ternary complex of CRP, LacR, and P*lac* DNA *in vitro*, with the simultaneous presence of LacR and cAMP–CRP increasing the affinity of both proteins for their respective binding sites by a cooperative factor (Ω) of 4- to 12-fold.

To see whether CRP-assisted DNA looping may quantitatively explain the observed codependency of P*lac* activity, we extended the thermodynamic model with DNA looping to include the CRP-dependent looping effect (*SI Methods*). The extended model predicts the IPTG response to have the same form as Eq. **3** but with the prefactor α_0 replaced by the Hill function α_{cAMP} for strain TK310 (Eq. **2** with parameters given by Table 2, row 2) and with the loop parameter L_0 replaced by

$$L = L_0 \cdot \frac{1 + \Omega \cdot [cAMP]/C_{cAMP}}{1 + [cAMP]/C_{cAMP}}, \quad [5]$$

where Ω is the cooperativity factor of the CRP–LacR–loop interaction.

To test the predictions of the extended thermodynamic model, we used Eq. **4** to infer the value of the loop parameter L from the maximal fold-change of the IPTG response at each cAMP value; the result is plotted as the circles in Fig. 2*a*. We then used Eq. **3** to compute the expected IPTG responses using these values of L. The results are shown as the dashed lines in Fig. 2*b* for several representative cAMP values, together with the experimental data for TK310 cells grown in media with the corresponding cAMP concentrations. Note that the dashed lines are not fits of the data to the model. The striking congruence between the dashed lines and the data points (for [cAMP] ≤ 1 mM) shows that the cAMP-dependent sensitivity, which requires a series of different Hill coefficients within the Hill function description (SI Fig. 5*a*), can be naturally described by the DNA looping model in terms of the cAMP-dependent loop parameter L with no other adjustable parameters.

[¶]We note that the increased in cooperativity by DNA looping was discussed recently by Vilar and Saiz (75) in the context of the lysis-lysogeny control of Phage λ. However, the mechanism of cooperativity there is the oligomerization of regulatory proteins made possible through DNA looping. In contrast here, the tetramerization of LacR is independent of DNA looping. What DNA looping enhances here is the sensitivity to IPTG rather than LacR.

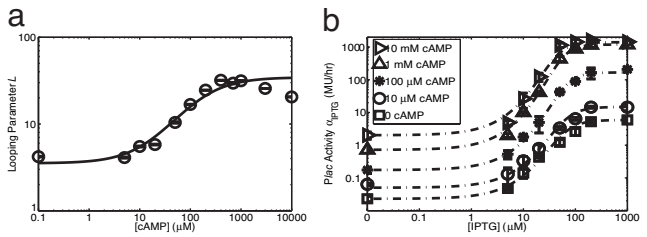

Fig. 2. Combinatorial control of P*lac* activity for strain TK310. (*a*) The cAMP-dependent loop parameter L is inferred from Eq. **4** by fixing the maximal fold-change f_{IPTG} to be the ratio of α_0 and the observed promoter activity in medium with no IPTG. α_0 is generated by the bare cAMP response α_{cAMP} by using the parameters in Table 2 (row 2). The result obtained (circles) is fitted to Eq. **5** by using a single fitting parameter, $\Omega = 10.3 \pm 0.1$, with $C_{cAMP} = 320$ μM (Table 2, row 2) and $L_0 = 3.7$ (Table 3, row 4). (*b*) The IPTG responses obtained at different cAMP levels (symbols) are plotted together with predictions of the CRP-assisted DNA-looping model (Eq. **3**) with no adjustable parameters. We used $R = 50$ and $K_{IPTG} = 12.3$ μM (Table 3, row 3), with values of L taken from *a* and α_{cAMP} for α_0 (Eq. **2** with parameters values given in Table 2, row 2).

To further examine whether the cAMP-dependence of L conforms to the known energetics of CRP-assisted DNA looping, we fitted the inferred values of L (Fig. 2*a*, circles) to Eq. **5** by allowing only the parameter Ω to vary. The result of the fit (Fig. 2*a*, solid line) described the data well, except again at the highest cAMP level (10 mM), where cell growth significantly slowed down and other effects (e.g., overexpression of nucleoid proteins) might significantly affect DNA bending and looping (70). The value of the best-fit parameter obtained, $\Omega = 10.3 \pm 0.1$, is in agreement with the 4- to 12-fold cooperativity found *in vitro* (*SI Methods*) (31, 33). SI Fig. 6*b* shows the 3D plot of the expected P*lac* activity according to the extended thermodynamic model. Collectively, these results provide strong quantitative support for the hypothesis of CRP-assisted repression by DNA looping (31–33).

Finally, we repeated the analysis for the combinatorial control of TK250 cells which are *cpdA*$^+$. Despite the unexpected cooperative nature of the cAMP response of this strain (Fig. 1*b*, blue symbols), with $m_{cAMP} \approx 2$, the IPTG responses at various cAMP levels (SI Fig. 10*b*) are still well described by Eq. **3** (with the best-fit values of K_{IPTG} and L_0 given in Table 3, row 3). Moreover, except for the highest cAMP concentrations again, the cAMP-dependence of the loop parameter L agrees well with the corresponding Hill function, with similar value of the cooperativity factor, $\Omega \approx 9.7$ (see SI Fig. 10*a*). These results indicate that *cpdA* expression affects only the activation of CRP by extracellular cAMP but not the interaction of cAMP–CRP with DNA looping itself.

Discussion

Systematic, quantitative characterization of gene expression may yield unique insights on the mechanisms of gene regulation. A major obstacle in this effort is to quantify the amount of active transcription factors in cells in a given environment. As attempted earlier by Setty *et al.* (28), we tackled this problem for the P*lac* by controlling the amount of inducers IPTG and cAMP extracellularly but with the *cyaA* mutant of *E. coli*, which cannot synthesize cAMP endogenously. One danger of this approach is the array of mechanisms the cell may employ to control the intracellular effector levels. We encountered two such mechanisms in our study. Through the positive feedback of the Lac permease, *E. coli* cells sensitize themselves to the presence of inducers of the LacR, whereas through the activity of PDE, *E. coli* cells appear to insulate themselves from low levels of cAMP in the environment. The LacY effect is well known for induction with lactose in the growth medium (16, 17). However, the PDE effect observed here is previously unknown. It may yield important clues toward a comprehensive understanding of cAMP transport and control central to carbon metabolism in *E. coli*.

DNA Looping Is Assisted by CRP. The innate regulation of P*lac* activity is revealed in *E. coli* cells bearing *cyaA lacY cpdA* triple deletion. We found that with a saturating amount of IPTG in the medium, the cAMP–CRP-mediated activation behaved in accordance with the thermodynamic model, given the noncooperative nature of the cAMP–CRP interaction. In addition, in the absence of cAMP, the LacR-mediated repression behaved in accordance with the thermodynamic model with DNA looping. Moreover, the codependence on IPTG and cAMP can be explained by the extended thermodynamic model with a single cooperativity parameter, Ω, whose value is of the order found by *in vitro* experiments. Both the quality of the fit and the simplicity of the model (i.e., one parameter for codependence) are superior compared with other simple but ad hoc models, as we show explicitly in SI Fig. 8). These results strongly support the hypothesis of CRP-assisted DNA looping (29, 31) and shed light on the seemingly conflicting roles CRP plays in the regulation of the P*lac*: CRP is an activator in that it increases gene expression at each IPTG level. However, it increases gene expression in a nonlinear way such that the maximal fold-change and the sensitivity of the IPTG response are both enhanced.

Hypersensitivity of IPTG Response Resulted from Multiple Factors. Even in the absence of *lacY*-mediated feedback, P*lac* activity depended sensitively on the IPTG level with an apparent Hill coefficient of 2.5~3 at physiological intracellular cAMP concentrations. This is rather remarkable given that the basic interaction of IPTG with the Lac tetramer is not cooperative at all in the absence of operator DNA (24). Whereas the involvement of DNA looping in the IPTG hypersensitivity is shown qualitatively by the experiment of Oehler *et al.* (62), the results and analysis of this study reveal the complex way in which this hypersensitivity is attained. First, the noncooperative IPTG–LacR binding becomes weakly cooperative (effective Hill coefficient of ≈1.5) in the presence of operator DNA (SI Fig. 7) (22–25), due presumably to the allosteric coupling between inducer and operator binding (see *SI Methods*). The involvement of DNA looping then increases the cooperativity (effective Hill coefficient of ≈2), because both dimeric units of the Lac tetramer are required to bind specifically to operators to form DNA loops. Finally, in the physiological range of intracellular cAMP concentrations where CRP is activated, the cooperative interplay between DNA looping and CRP-mediated DNA bending further enhances the looping-induced cooperativity to the observed effective Hill coefficient of 2.5~3.

As shown by Novick and Weiner (16) and by Ozbudak *et al.* (17), the hypersensitivity of P*lac* activity to the inducer of LacR is crucial for the bistable (i.e., the all-or-none) nature of *E. coli*'s lactose utilization strategy (16, 17). The latter is the molecular basis of important physiological effects, such as the diauxie shift (71). It is interesting that hypersensitivity resulted in this case from an agglomeration of weak interactions. This distributed way of implementing an important molecular function (instead of, e.g., a highly cooperative LacR–inducer interaction) may reflect the serendipity of the evolutionary dynamics or, alternatively, a robust evolutionary strategy to preserve important system-level functions.

The Importance of Being Quantitative. Critical to this study was the recognition of various "artifacts" produced by processes not directly related to the regulation of the P*lac*. The key discriminating feature we used was the quantitative comparison of the observed responses to the expectations of the thermodynamic model, in light of the known biochemical processes. Although fitting the experimental data to a Hill form is in itself not a very discriminating task, we find that the "reasonableness" of the numerical values of the fitting parameters, especially the apparent Hill coefficients of the re-

sponses, can be quite revealing. Nevertheless, the power of the quantitative analysis is by itself limited, because it can only suggest the existence of problems but does not identify the sources. It is through the quantitative comparison of the characteristics of a series of key mutants that the major conclusions of this study are established. It is important to note that some of our most discriminating mutants did not display much difference in the high/low states of expression but exhibited clear differences in the abruptness of the transition between states.

The P*lac* is one of the prototypical model systems of gene regulation. Classic studies on the regulation of this promoter have established numerous fundamental concepts as well as laying down the appropriate methodology for studying the molecular biology of gene regulation. Quantitative studies of the P*lac* can again play important roles in laying down the foundation of quantitative systems biology, whose goal is to understand the behavior of a "system" in terms of the relevant properties of its components. The P*lac* is admittedly a rather simple system. Nevertheless, we see from this study that system-level properties, such as the sensitivity of the IPTG response, resulted from a closely intertwined set of interactions among the molecular constituents. We demonstrated how this system can be dissected by careful quantitative characterization and targeted genetic manipulations, along with guidance from quantitative modeling and the knowledge of the biochemistry of the molecular constituents. The experience gained here may be of value to the study of other more complex biological systems.

Methods

Plasmids and Strains. All strains used in this study were derived from *E. coli* K-12 MG1655 as listed in SI Table 4 and detailed in *SI Methods*. Chromosomal gene deletion was performed by using the method of Datsenko and Wanner (71), and transferred from one strain to another by using P1 transduction. All mutations were verified with PCR.

Cell Growth and β-Galactosidase Assay. Overnight cultures were grown in M9 minimal medium containing the standard concentrations of necessary antibiotics in a 37°C water bath until stationary phase. The carbon source was 0.5% glucose unless otherwise indicated. These cultures were diluted 100- to 1,000-fold into 24-well plates (Costar) containing the same growth medium plus various concentrations of IPTG and cAMP. The plates were grown with vigorous shaking in a humidity-controlled incubator maintained at 37°C, with OD_{600} measurements taken every 2 h in a Tecan Genios Pro plate reader. When OD_{600} of a sample reached 0.2–0.4, it was assayed for β-galactosidase activity. These assays were performed in triplicate or more according to Miller (73) and Griffith (74), with minor modifications detailed in *SI Methods*. The β-galactosidase activity obtained (A) was expressed in Miller units (73), and the promoter activity (α) reported was taken to be the product of A and the cell-doubling rate $\lambda_{1/2}$. Serial dilution experiments were used to verify that the entire range of promoter activity reported in the figures lay within the linear responsive regime of the measurements (see *SI Methods*).

We thank Bob Schleif, Bill Loomis, and Shumo Liu for pointing out conceptual flaws in early versions of our experiments and Nicolas Buchler, Antoine Danchin, Hernan Garcia, Kathleen Matthews, Stefan Oehler, Rob Philips, and Agnes Ullmann for valuable comments. This work was supported by Department of Energy Grant DE-FG02-03-ER63691, National Science Foundation Grant MCB-0417721, and National Institutes of Health Grant GM070915. T.K. and T.H. were supported by Center for Theoretical Biological Physics Grants PHY-0216576 and PHY-0225630 through the National Science Foundation Physics Frontier Centers program.

1. Monod J (1947) *Growth* 11:223–289.
2. Beckwith J (1987) in *Escherichia coli and Salmonella typhimurium: Cellular and Molecular Biology*, eds Neihardt JL, Ingraham KB, Low B, Magasanik B, Umbarger HE (Am Soc Microbiol, Washington, DC), Vol 2, pp 1439–1443.
3. Beckwith J, Grodzicker T, Arditti R (1972) *J Mol Biol* 69:155–160.
4. Gilbert W, Muller-Hill B (1970) in *The Lactose Operon*, eds Beckwith J, Zipser D (Cold Spring Harbor Lab Press, Plainview, NY), pp 93–109.
5. Muller-Hill B (1996) *The lac Operon* (de Gruyter, Berlin).
6. Oehler S, Amouyal M, Kokhof P, von Wilcken Bergmann B, Muller-Hill B (1994) *EMBO J* 13:3348–3355.
7. Davidson EH, Rast JP, Oliveri P, Ransick A, Calestani C, Yuh CH, Minokawa T, Amore G, Hinman V, Arenas-Mena C (2002) *Science* 295:1669–1678.
8. Buchler NE, Gerland U, Hwa T (2003) *Proc Natl Acad Sci USA* 100:5136–5141.
9. Epstein W, Rothman-Denes LB, Hesse J (1975) *Proc Natl Acad Sci USA* 72:2300–2304.
10. Saier MH, Jr (1989) *Microbiol Rev* 53:109–120.
11. Saier MH, Jr, Feucht BU, McCaman MT (1975) *J Biol Chem* 250:7593–7601.
12. Aboud M, Burger M (1970) *Biochem Biophys Res Commun* 38:1023–1032.
13. Contesse M, Crepin M, Gros F, Ullmann A, Monod J (1970) in *The Lactose Operon*, eds Beckwith JR, Zipser D (Cold Spring Harbor Lab Press, Plainview, NY), pp 401–416.
14. Pastan I, Perlman R (1970) *Science* 169:339–344.
15. Makman RS, Sutherland EW (1965) *J Biol Chem* 240:1309–1314.
16. Novick A, Weiner M (1957) *Proc Natl Acad Sci USA* 43:553–566.
17. Ozbudak EM, Thattai M, Lim HN, Shraiman BI, Van Oudenaarden A (2004) *Nature* 427:737–740.
18. Zubay G, Schwartz D, Beckwith J (1970) *Proc Natl Acad Sci USA* 66:104–110.
19. Eismann E, von Wilcken-Bergmann B, Muller-Hill B (1987) *J Mol Biol* 195:949–952.
20. Eismann ER, Muller-Hill B (1990) *J Mol Biol* 213:763–775.
21. Oehler S, Eismann ER, Kramer H, Muller-Hill B (1990) *EMBO J* 9:973–979.
22. Muller J, Oehler S, Muller-Hill B (1996) *J Mol Biol* 257:21–29.
23. Friedman BE, Olson JS, Matthews KS (1977) *J Mol Biol* 111:27–39.
24. Chen J, Alberti S, Matthews KS (1994) *J Biol Chem* 269:12482–12487.
25. O'Gorman RB, Rosenberg JM, Kallai OB, Dickerson RE, Itakura K, Riggs AD, Matthews KS (1980) *J Biol Chem* 255:10107–10114.
26. Daly TJ, Matthews KS (1986) *Biochemistry* 25:5479–5484.
27. Yagil G, Yagil E (1971) *Biophys J* 11:11–27.
28. Setty Y, Mayo AE, Surette MG, Alon U (2003) *Proc Natl Acad Sci USA* 100:7702–7707.
29. Busby S, Ebright RH (1999) *J Mol Biol* 293:199–213.
30. Lewis M, Chang G, Horton NC, Kercher MA, Pace HC, Schumacher MA, Brennan RG, Lu P (1996) *Science* 271:1247–1254.
31. Balaeff A, Mahadevan L, Schulten K (2004) *Structure (London)* 12:123–132.
32. Fried MG, Hudson JM (1996) *Science* 274:1930–1931, and author reply (1996) 274:1931–1932.
33. Hudson JM, Fried MG (1990) *J Mol Biol* 214:381–396.
34. Vossen KM, Stickle DF, Fried MG (1996) *J Mol Biol* 255:44–54.
35. Bintu L, Buchler NE, Garcia HG, Gerland U, Hwa T, Kondev J, Kuhlman T, Phillips R (2005) *Curr Opin Genet Dev* 15:125–135.
36. Bintu L, Buchler NE, Garcia HG, Gerland U, Hwa T, Kondev J, Phillips R (2005) *Curr Opin Genet Dev* 15:116–124.
37. Ackers GK, Johnson AD, Shea MA (1982) *Proc Natl Acad Sci USA* 79:1129–1133.
38. Monod J (1956) in *Enzymes: Units of Biological Structure and Function* (Academic, New York), pp 7–28.
39. Jensen PR, Westerhoff HV, Michelsen O (1993) *Eur J Biochem* 211:181–191.
40. Vilar JM, Saiz L (2005) *Curr Opin Genet Dev* 15:136–144.
41. Ide M (1969) *Biochem Biophys Res Commun* 36:42–46.
42. Perlman RL, Pastan I (1969) *Biochem Biophys Res Commun* 37:151–157.
43. Tao M, Lipmann F (1969) *Proc Natl Acad Sci USA* 63:86–92.
44. Magasanik B (1970) in *The Lactose Operon*, eds Beckwith J, Zipser D (Cold Spring Harbor Lab Press, Plainview, NY), pp 189–219.
45. Magasanik B, Neidhardt F (1987) in *Escherichia coli and Salmonella typhimurium: Cellular and Molecular Biology*, ed Neidhardt F (Am Soc Microbiol, Washington, DC), Vol. 2, pp 1325–1343.
46. Ullmann A, Danchin A (1983) *Adv Cyclic Nucleotide Res* 15:1–53.
47. Crasnier-Mednansky M, Park MC, Studley WK, Saier MH, Jr (1997) *Microbiology* 143:785–792.
48. Krin E, Sismeiro O, Danchin A, Bertin PN (2002) *Microbiology* 148:1553–1559.
49. Takahashi M, Blazy B, Baudras A, Hillen W (1989) *J Mol Biol* 207:783–796.
50. Fried MG, Crothers DM (1984) *J Mol Biol* 172:241–262.
51. Garner MM, Revzin A (1982) *Biochemistry* 21:6032–6036.
52. Harman JG (2001) *Biochim Biophys Acta* 1547:1–17.
53. Aboud M, Burger M (1971) *Biochem Biophys Res Commun* 43:174–182.
54. Brana H, Chytil F (1965) *Folia Microbiol* 11:43–46.
55. Monard D, Janecek J, Rickenberg HV (1969) *Biochem Biophys Res Commun* 35:584–591.
56. Nielsen LD, Monard D, Rickenberg HV (1973) *J Bacteriol* 116:857–866.
57. Nielsen LD, Rickenberg HV (1974) *Methods Enzymol* 38:249–256.
58. Imamura R, Yamanaka K, Ogura T, Hiraga S, Fujita N, Ishihama A, Niki H (1996) *J Biol Chem* 271:25423–25429.
59. Gerland U, Moroz JD, Hwa T (2002) *Proc Natl Acad Sci USA* 99:12015–12020.
60. Straney DC, Straney SB, Crothers DM (1989) *J Mol Biol* 206:41–57.
61. Malan TP, Kolb A, Buc H, McClure WR (1984) *J Mol Biol* 180:881–909.
62. Oehler S, Alberti S, Muller-Hill B (2006) *Nucleic Acids Res* 34:606–612.
63. Nichols JC, Matthews KS (1997) *J Biol Chem* 272:18550–18557.
64. Jobe A, Bourgeois S (1972) *J Mol Biol* 69:397–408.
65. Fried MG, Daugherty MA (2001) *J Biol Chem* 276:11226–11229.
66. Perros M, Steitz TA (1996) *Science* 274:1929–1930, and author reply (1996) 274:1931–1932.
67. Borowiec JA, Zhang L, Sasse-Dwight S, Gralla JD (1987) *J Mol Biol* 196:101–111.
68. de Crombrugghe B, Busby S, Buc H (1984) *Science* 224:831–838.
69. Becker NA, Kahn JD, Maher LJ, III (2005) *J Mol Biol* 349:716–730.
70. Monod J (1950) *Ann Inst Pasteur* 79:390.
71. Datsenko KA, Wanner BL (2000) *Proc Natl Acad Sci USA* 97:6640–6645.
72. Lutz R, Bujard H (1997) *Nucleic Acids Res* 25:1203–1210.
73. Miller JH (1972) *Experiments in Molecular Genetics* (Cold Spring Harbor Lab Press, Plainview, NY).
74. Griffith KL, Wolf RE, Jr (2002) *Biochem Biophys Res Commun* 290:397–402.

SI METHODS

Experimental Methods

Plasmids and strains. *E. coli* K-12 MG1655 and derived mutants were used in all experiments reported in the main text. Chromosomal deletions were performed using the method of Datsenko & Wanner (1). For each deletion the kanamycin resistance gene *kan* was amplified from the template plasmid pKD4 using primer sites P0 and P2 including 45 bp homology extensions. The PCR products were then transformed into electrocompetent MG1655 cells, and *kan* was eliminated using plasmid pCP20 bearing FLP recombinase (1). The resulting strains TK110, TK120, TK130, TK140, and TK150 are listed in Table S1 together with the start and end coordinates of the respective deletions. All mutations were verified using PCR. Multiple deletion strains were constructed by serially transferring and eliminating the TK100 series of *kan* insertion mutants into the target strain using P1 transduction in the order indicated in column 3 of SI Table 4, with the exception of strain TK200 carrying Δ*lacI* Δ*lacY* double mutation. The close proximity of *lacI* to *lacY* necessitated the *de novo* synthesis of both mutations in the same host strain.

Measurements of the variation of CRP levels were performed on strain TK500. This strain was derived from strain TK400, which was derived in turn from *E. coli* BW25113 (1), with *cyaA* deletion performed as explained above. The *crp* promoter P*crp* was amplified from MG1655 genomic DNA from start coordinate 3483424 to end coordinate 3483721 and inserted into the EcoRI and BamHI sites of PRS551 (2). The resulting P*crp-lacZ* fusion was inserted into the chromosome of TK400 using the method of Simons *et al*. (2). Measurements of the effect of the CRP operator on the *lac* promoter were performed using strain TK600 which is also derived from strain TK400. The *lac* promoter was amplified from start coordinate 365438 to end coordinate 365669 and cloned into the EcoRI and BamHI sites of pRS551. The CRP operator site at position -61.5 was altered from TGTGAGTTAGCTCACT to CAGACGTTAGCTCACT using site-directed mutagenesis (Stratagene) and the resulting construct was inserted into the chromosome of strain TK400 using the method of Simons *et al*. (2).

β-Galactosidase assay. Assays of β-galactosidase activity were performed according to Miller (3) and Griffith and Wolf (4) with changes as follows. Overnight cultures of bacterial strains were grown in 3ml M9 minimal medium (M9, 1 mM $MgSO_4$, 0.1 mM $CaCl_2$) containing 0.5% glucose as the sole carbon source and the standard concentrations of any necessary antibiotics in

a 37°C water bath until saturation. This culture was diluted[†] into 24-well plates (Costar) containing 1ml M9 medium in each well with glucose, antibiotics, and varying concentrations of 3',5'-cyclic adenosine monophosphate (cAMP) (0-10 mM) and isopropyl β-D thiogalactopyranoside (IPTG) (0-1 mM). The plates were then grown with vigorous shaking at 200 rpm in a humidity-controlled incubator, with OD_{600} measurements taken every two hours in a Tecan Genios Pro plate reader. The cell-doubling rate ($\lambda_{\frac{1}{2}}$) for each sample was calculated as the slope of $\log_2(OD_{600})$ vs. time plot via linear regression analysis.

When OD_{600} of a sample reaches 0.2-0.4, 0.5 ml of the sample was transferred to a 2-ml 96 well polypropylene block containing 0.5 ml Z-buffer (3), 20 µl 0.1% SDS, and 40 µl chloroform. All samples were thoroughly disrupted by repeated agitation with a multichannel pipettor. 200 µl of each sample was transferred to a flat-bottom transparent 96 well plate (Costar). 40 µl of Z-buffer containing 4 mg/ml *o*-nitrophenyl-β-D-galactopyranoside (ONPG) was added to each well and OD_{420} measurements were performed in a Tecan Genios Pro plate reader, at 1-minute intervals for the first 10 minutes, and at increasing intervals (1 hour, 5 hour, etc.) thereafter[‡] until sufficient color had developed in all samples for measurement, and the measured OD_{420} showed an extended regime of linear dependence on time (data not shown). Samples were maintained at 25°C throughout incubation. All assays were performed in triplicate or more.

Promoter activity. In the regime where the OD_{420} readings were sufficiently large to ensure a linear dependence on time of measurements but below 1.0 (above which the OD_{420} readings saturate), the slope (s) of OD_{420} versus time (in minutes) was calculated via linear regression. β-galactosidase activity (A) was expressed in Miller Units (MU) according to the formula $A = (1000 \cdot s) / (0.5 \cdot \mathrm{OD}_{600})$. To verify the reliability of the deduced activity for the weakly expressed promoters, we performed a serial dilution experiment, using MG1655 grown in M9 medium with 0.5% glucose and 1 mM IPTG, which yielded a β-galactosidase activity of ~1000 MU. We mixed this strain with strain BW25113, deleted of the *lac* operon, in varying

[†] In M9 medium, the growth rate of Δ*cyaA* strains increases from 0.4 doubling/hour at 0 cAMP to a maximum of 0.6 doubling/hour at ~1 mM cAMP; see SI Fig. 4*a*. As such, the initial inoculation of samples was performed at different dilutions (~1000x dilution for samples in 1 mM cAMP and ~ 100x dilution for samples at lower cAMP concentrations) such that all samples would reach OD_{600} = 0.2-0.4 in approximately 12-15 hours. We verified that samples assayed with various initial dilutions in the given range gave no measurable systematic variations in results (data not shown).

[‡] For the lowest expression encountered in the experiments performed (e.g., the *crp* null mutants in Fig. 1*a*), this took up to 50 hours.

proportions (up to 10^6-fold dilution), and measured the apparent β-galactosidase activity of the mixture using the procedure specified above. We found a nearly perfect inverse dependence of the observed β-galactosidase activity with the fold-dilution applied down to ~0.03 MU (data not shown). As the lowest β-galactosidase activity encountered in the experiments was ~0.1 MU, our data lay completely in the responsive regime of the measurements.

In the text, we report the "promoter activity" (α) as

$$\alpha = A \cdot \lambda_{\frac{1}{2}}, \qquad \textbf{[6]}$$

where $\lambda_{\frac{1}{2}}$ is the cell-doubling rate defined above (in unit of 1/hr). This measure of the promoter activity is motivated by the fact that the enzyme β-galactosidase is very stable (5) so that in the balanced exponential growth phase, its "turnover" is governed by dilution due to cell growth; see discussion below. Note that with the definition Eq. **6**, we take into account some straightforward growth-dependent effects on β-galactosidase activity as previously reported (6, 7). There are of course other residual effects, e.g., variation in the cellular levels of RNA polymerase, ribosomes, etc at the different growth rates. However, these effects are apparently quite limited in magnitude and will be neglected in our analysis: As seen in SI Fig. 4*b* (triangles), the growth-rate adjusted activity of β-galactosidase expressed by the (constitutive) P*lacΔcrp* promoter in *cyaA*- cells changed very little in growth medium with various cAMP concentrations, even though the growth rate itself changed appreciably over this range of cAMP concentrations (SI Fig. 4*a*).

Theoretical Modeling. *Activation of the regulatory proteins.*

The concentrations of the active regulators are controlled by the total concentrations of the regulators, the intracellular inducer concentrations, and the biochemistry of inducer-regulator interaction. The interaction of CRP with cAMP is quite straightforward (8-11) and will be discussed first. The active component is the CRP dimer associated with one cAMP molecule (10-12). For simplicity, we will assume that all the CRP monomers associate in the dimer form, as justified by the very small dimer dissociation constant [0.1 – 1 nM; (13)] The concentration of the activated CRP dimer (denoted by $[CRP^*]$) is then given by

$$\left[CRP^*\right] \equiv [cAMP - CRP] = [CRP] \cdot \frac{[cAMP]^*_{in}}{[cAMP]^*_{in} + K_{cAMP}}, \quad \textbf{[7]}$$

where [CRP] denotes the total CRP dimer concentration, $K_{cAMP} = 10\ \mu$M is the relevant dissociation constant (10), and $[cAMP]^*_{in}$ is the intracellular concentration of cAMP. Intracellular cAMP is believed to be rapidly exported by PMF pumps (14, 15). For *cyaA* strains which cannot synthesize cAMP endogenously, the high export/import ratio leads to a much smaller intracellular cAMP concentration compared to the extracellular concentration. It is this intracellular cAMP concentration which dictates the degree of CRP activation (assuming that cAMP-CRP equilibration is much faster than cAMP transport.) The details of cAMP transport are not understood; even the cAMP pump has not been identified despite many years of study. Here, we appeal to the results of Epstein *et al*. (16) and assume that the intracellular cAMP concentration is linearly related to the extracellular concentration across the range of concentrations used, i.e., $[cAMP]^*_{in} = \gamma_{cAMP} \cdot [cAMP]$, where [cAMP] is the cAMP level of the medium. Since $\gamma_{cAMP} \approx 10^{-3}$ according to ref. 16, we have $[cAMP]^*_{in} = \gamma_{cAMP} \cdot [cAMP] = K_{cAMP}$ for most of the range of cAMP used in our experiment (0 – 10 mM). Hence Eq. **7** is simplified to

$$\left[CRP^*\right] \approx [CRP] \cdot [cAMP] \cdot \gamma_{cAMP} / K_{cAMP}. \quad \textbf{[8]}$$

Obtaining the active concentration of the Lac repressor is more involved. The Lac repressor is a dimer of dimers (17). Co-crystal structure of LacR and operator DNA indicates that the dimer binds specifically to the operator sequence as a unit in the absence of IPTG, while the IPTG-bound dimers do not have the required structure to bind specifically to operator DNA. Additionally, since the two dimeric units of the LacR tetramer interact very weakly (18), we do not expect the IPTG binding by one dimeric unit to affect the specific DNA binding of the other dimeric unit. Finally, we do not expect a dimeric unit to be able to bind specifically to operator sites if either one of its monomeric subunit is bound to IPTG. This assumption is based on the work of Winter, Berg, and von Hippel (19), who showed that sequence specific binding would only occur if the energy gained from sequence-specific binding more than compensates the loss of electrostatic energy the repressor molecule could gain in a conformation that does not allow specific DNA binding. When one of the monomers bind to IPTG, that monomer could not contribute to specific DNA binding, and the other monomer would not be able to contribute

enough to compensate given what we know about the energetics of LacR-DNA binding (19). The last feature described above, that both monomers of a dimeric unit need to be free of IPTG binding in order for the dimeric unit to bind specifically to operator DNA, is a crucial source of cooperativity in our model. While there is no direct biochemical proof of this feature, we mention that a MWC model incorporating this feature of LacR-DNA binding (T.K. and T.H., unpublished data) is able to reproduce the effective Hill coefficient of 1.4 ~ 1.6 which describes the IPTG dependence of specific operator binding, as observed in the experiments of O'Gorman *et al*. (20). It then follows that there are two species of "active repressors" in our model: (*i*) Only one of the two dimeric units is not bound at all by IPTG (denoted by LacR*), and (*ii*) neither of the dimeric units is bound by IPTG (denoted by LacR**).

To find the concentrations of these two active species (denoted by $[LacR^{*}]$ and $[LacR^{**}]$ respectively) in terms of the total LacR tetramer concentration [LacR] and the IPTG concentration $[IPTG]$, we need to keep track of all possible molecular species of LacR-IPTG complex. As illustrated in SI Fig. 11, there is one species with no IPTG (denoted by LacR-0), four sub-species with one IPTG bound (LacR-1), two sub-species with two IPTG bound to a single dimer (LacR-2a), four sub-species with two IPTG bound to two different dimers (LacR-2b), four subspecies with three IPTG bound (LacR-3) and one subspecies with four IPTG bound (LacR-4). Since the IPTG-LacR binding is non-cooperative (20), the equilibrium between any two subspecies linked by a line in SI Fig. 11 is described by the same dissociation constant K_{IPTG}. Taking into account of the indistinguishability of the subspecies, we arrive at the following equilibrium relations among the species of LacR-IPTG complex:

$$\frac{[LacR-1]}{[LacR-0]}=\frac{4[IPTG]}{K_{IPTG}};\ \frac{[LacR-2a]}{[LacR-0]}=2\cdot\left(\frac{[IPTG]}{K_{IPTG}}\right)^{2};\frac{[LacR-2b]}{[LacR-0]}=4\cdot\left(\frac{[IPTG]}{K_{IPTG}}\right)^{2};$$

$$\frac{[LacR-3]}{[LacR-0]}=4\cdot\left(\frac{[IPTG]}{K_{IPTG}}\right)^{3};\ \frac{[LacR-4]}{[LacR-0]}=\left(\frac{[IPTG]}{K_{IPTG}}\right)^{4}.$$

Since the total LacR concentration is the sum of the concentrations of the individual species, we have

$$\left[LacR^{**}\right]\equiv[LacR-0]=[LacR]\Big/\left(1+[IPTG]/K_{IPTG}\right)^{4} \qquad \textbf{[9]}$$

and

$$\left[LacR^*\right] \equiv [LacR-1]+[LacR-2a] = [LacR]\cdot \frac{4\left([IPTG]/K_{IPTG}\right)+2\left([IPTG]/K_{IPTG}\right)^2}{\left(1+[IPTG]/K_{IPTG}\right)^4}. \quad \textbf{[10]}$$

Thermodynamic modeling. The transcriptional activity of a given promoter controlled by the binding and interaction of transcription factors (TF) can be modeled using a generalized Shea-Ackers like thermodynamic model (21) as described in Buchler *et al*. (22) and Bintu *et al.* (23, 24). Briefly, we assume that the rate of protein expression, *G*, is proportional to the equilibrium probability *P* of the RNA polymerase (RNAP) binding to its DNA target, the promoter, given the cellular concentrations of all of the relevant transcript factors. The probability *P* can be written as

$$P = \frac{Z_{ON}}{Z_{ON}+Z_{OFF}},$$

where Z_{ON} and Z_{OFF} are the partition sums of the Boltzmann weights over all states of transcription factor binding for the promoter bound and not bound, respectively, by the RNA polymerase. Given the knowledge of the cellular concentrations of the TFs, the partition function of the TFs themselves (Z_{OFF}) is simply

$$Z_{OFF} = \sum_{all\ \sigma_i=\{0.1\}} \prod_{(i,j)} \left(\frac{[TF_{s(i)}]}{K_i}\right)^{\sigma_i} \cdot \left(\frac{[TF_{s(j)}]}{K_j}\right)^{\sigma_j} \cdot \omega_{i,j}^{\sigma_i\sigma_j}, \quad \textbf{[11]}$$

where K_i refers to the dissociation constant of operator site i with its TF [of type *s* as indicated by subscript $s(i)$], and $\omega_{i,j}$ is the cooperativity factor between the two TFs bound to operator sites *i* and *j*. It is important to note that K_i is the effective *in vivo* binding constant including the effect of binding of its TF to all other possible binding sites on the chromosome, and is typically not the value of *in vitro* measurement (25). The values of the $\omega_{i,j}$ depend on the spacing between sites *i* and *j*. If two sites are overlapping, $\omega_{i,j}=0$, reflecting the fact that they cannot be simultaneously occupied. If two sites are positioned such that the two bound TFs can not contact each other, then $\omega_{i,j}=1$, indicating the lack of interactions between the bound TFs. For two TFs that can bind cooperatively and their binding sites are positioned such that the bound TFs do interact, then the value of $\omega_{i,j}$ is the cooperativity factor of that interaction, and is typically of the order 10~100 (22). The expression for Z_{ON} is similar to Eq. **11**, but with one of the sites being the promoter, and one of the [TF_s] being [RNAP].

As an example, consider a promoter with a single binding site for an activator protein *A*, which binds to its site with dissociation constant K_A and interacts with RNAP via a cooperativity factor $\omega > 1$. The equilibrium promoter occupation probability *P* can then be written as

$$P = \frac{[RNAP]/K_{RNAP} \cdot (1 + \omega \cdot [A]/K_A)}{1 + [A]/K_A + [RNAP]/K_{RNAP} \cdot (1 + \omega \cdot [A]/K_A)} \cong \frac{[RNAP]}{K_{RNAP}} \cdot \frac{1 + \omega \cdot [A]/K_A}{1 + [A]/K_A}$$

where the approximation above is justified by the fact that typical core promoters are very weak such that $[RNAP]/K_{RNAP} \ll 1$ (22-24). The rate of protein expression, $G \propto P$, can then be written as

$$G \approx G_0 \cdot \frac{1 + \omega \cdot [A]/K_A}{1 + [A]/K_A}. \quad \textbf{[12]}$$

where G_0 is a basal protein expression rate, involving the rate of transcription, translation as well as mRNA turnover, in the absence of any regulatory proteins. It is not a number computable from the thermodynamic model; on the other hand, the knowledge of this overall prefactor is not necessary for characterizing the relative effect of transcriptional control.

In the case of a repressor protein *R* which binds to its operator with dissociation constant K_R and precludes RNAP binding at the core promoter, the transcription rate can be written as

$$P = \frac{[RNAP]/K_{RNAP}}{1 + [R]/K_R + [RNAP]/K_{RNAP}} \; ; \; \frac{[RNAP]}{K_{RNAP}} \cdot \frac{1}{1 + [R]/K_R}$$

and the rate of protein expression as

$$G \approx G_0 \cdot \frac{1}{1 + [R]/K_R}. \quad \textbf{[13]}$$

For a promoter which is controlled by both a repressor and an activator, the simplest case would be that the two exert their influence on the RNAP independently and do not interact with each other. In this case, the combined response would simply be the product of the two expressions given above, i.e.,

$$G \approx G_0 \cdot \left(\frac{1 + \omega \cdot [A]/K_A}{1 + [A]/K_A} \right) \cdot \left(\frac{1}{1 + [R]/K_R} \right). \quad \textbf{[14]}$$

Below, we apply the general thermodynamic to the *lac* promoter.

Activation by cAMP-CRP. We first address activation by cAMP-CRP, whose concentration is $[CRP^*]$ as given by Eq. **8**. cAMP-CRP binds to the operator site at position -61.5 (see SI Fig. 9) and recruits the RNA polymerase to the core promoter. In the absence of LacR, this is just the case of "simple activation" considered in Eq. **12**. Denoting the *in vivo* binding constant (25) of cAMP-CRP to the operator site by K_{CRP}, and the cooperativity factor of CRP-RNAp interaction by ω, then the rate of LacZ synthesis is

$$G = G_0 \cdot \frac{1 + \omega \cdot [CRP^*] / K_{CRP}}{1 + [CRP^*] / K_{CRP}} . \qquad \textbf{[15]}$$

where G_0 is the same basal rate introduced in Eq. **12**. Eq. **15** describes the rate of LacZ synthesis. What we measure is the enzymatic activity (A) of LacZ (see *Methods* and *SI Methods*, section *Promoter activity*) in the steady state of balanced exponential growth. We take A to be proportional to the steady-state LacZ concentration $[LacZ]^*$. The latter is given through the kinetic equation

$$\frac{d}{dt}[LacZ] = G - \lambda \cdot [LacZ],$$

with the steady-state solution $G = \lambda \cdot [LacZ]^* \propto \lambda \cdot A$, where λ is the cell growth rate. In our study, we defined the promoter activity to be $\alpha \equiv A \cdot \lambda_{\frac{1}{2}}$ where $\lambda_{\frac{1}{2}} = \lambda / \ln 2$ is the doubling rate of the culture; see Eq. **6**. Hence, $G \propto \alpha$ as expected. Inserting the cAMP-dependence of $[CRP^*]$ as given by Eq. **8**, we have

$$\alpha_{cAMP} = b_0 \cdot \frac{1 + \omega \cdot [cAMP] / \kappa_{cAMP}}{1 + [cAMP] / \kappa_{cAMP}} , \qquad \textbf{[16]}$$

where $b_0 \propto G_0 \cdot \lambda$ and

$$\kappa_{cAMP} = K_{cAMP} \cdot K_{CRP} / [CRP] \cdot \gamma_{cAMP} . \qquad \textbf{[17]}$$

Eq. **16** is the Hill form used in the main text for the cAMP response (Eq. **2**), with $f_{cAMP} = \omega$, and $C_{cAMP} = \kappa_{cAMP}$. The predicted range for C_{cAMP} listed in Table 2 of the main text is obtained by using Eq. **17** with $K_{cAMP} = 10\ \mu$M (10), $K_{CRP} = 5 - 50$ nM (10), $\gamma_{cAMP} = 0.001$ (see discussion above), and $[CRP] = 1500$ nM (26).

Simple repression by LacR. Let us first consider the case of "simple repression" by the operator O1 alone (see SI Fig. 9), without the involvement of DNA looping and without activation by cAMP-CRP. In this case, repression is due solely to the direct steric interference between the binding of LacR to O1 and RNAp to the core promoter (17, 27, 28). Specifically, both activated species LacR* and LacR** can bind to O1 and block the promoter. Denoting the *in vivo* binding constant between either activated species and O1 by K_1, the rate of LacZ synthesis is given by Eq. **13** with $[R = [LacR^*] + 2[LacR^{**}]$, with the factor of 2 in the second term arising from the fact that there are two ways for LacR** to bind to O1. Thus,

$$G = G_0 \Big/ \left(1 + [LacR^*]/K_1 + 2\,[LacR^{**}]/K_1\right). \qquad \textbf{[18]}$$

Inserting into Eq. **18** the IPTG dependences of $[LacR^{**}]$ and $[LacR^*]$ as given by Eqs. **9** and **10**, we obtain the result

$$G = G_0 \Big/ \left(1 + \frac{2\,[LacR]/K_1}{\left(1 + [IPTG]/K_{IPTG}\right)^2}\right). \qquad \textbf{[19]}$$

Note that the factor $2[LacR]/\left(1 + [IPTG]/K_{IPTG}\right)^2$ in the denominator of Eq. **19** simply gives the concentration of the dimeric units of LacR tetramers which are not bound by IPTG.

The value of the factor $2\,[LacR]/K_1$ (denoted by R in the main text) can be inferred by noting that the degree of repression *f*, defined as the ratio of LacZ expression for cells grown in medium with saturating and zero IPTG, is simply given by $1 + R$ accord to Eq. **19**. Oehler *et al*. reported in a 1990 paper (29) that the degree of repression was ~20 for a mutant *lac* promoter containing only the operator O1. In a later paper (30), they reported degrees of repression of 200 and 4700 for the same mutant *lac* promoter in cells expressing 5x and 90x respectively of the amount of Lac tetramers of wildtype cells. These results yield an estimate of $R \approx 20$ or $R \approx 50$ for wildtype cells. In the following analysis we use $R \approx 50$, although results of similar quality are obtained for $R \approx 20$.

LacR-mediated DNA looping. To include repression due to DNA looping, we take into account of the additional possibility that a completely uninduced LacR tetramer (i.e., LacR**) may bind to two operator sites, the main operator O1 and one of the two auxiliary operator sites O2 or O3;

see SI Fig. 9. This is incorporated into the thermodynamic model by adding two looping terms[§] to the denominator of the expression in Eq. **18**, i.e.,

$$G = G_0 \Big/ \left(1 + \frac{[LacR^*]}{K_1} + \frac{2\,[LacR^{**}]}{K_1} + \frac{[LacR^{**}][L_{12}]}{K_1 K_2} + \frac{[LacR^{**}][L_{13}]}{K_1 K_3} \right) \qquad \textbf{[20]}$$

with K_2 and K_3 being the dissociation constant of the LacR tetramer with O2 and O3 respectively, and $[L_{12}]$ and $[L_{13}]$ describing the effective "local concentration" of the repressor at O2 and O3 respectively given that the tetramer is bound at O1; see refs. 22-24. The effective concentrations $[L_{12}]$ and $[L_{13}]$ involve the free energy cost of DNA looping and have not been directly characterized[**] by biochemical or biophysical methods for the *lac* promoter in the absence of CRP binding. Inserting again the IPTG-dependence of $[LacR^{**}]$, we obtain

$$G = G_0 \Big/ \left(1 + \frac{2\,[LacR]/K_1}{\left(1 + [IPTG]/K_{IPTG}\right)^2} + \frac{\left([LacR]/K_1\right)\cdot\left([L_{12}]/K_2 + [L_{13}]/K_3\right)}{\left(1 + [IPTG]/K_{IPTG}\right)^4} \right). \qquad \textbf{[21]}$$

As the P*lac* activity α is proportional to G (see above), we have

$$\alpha_{IPTG} = b_0 \Big/ \left(1 + \frac{R}{\left(1 + [IPTG]/K_{IPTG}\right)^2} + \frac{R \cdot L_0}{\left(1 + [IPTG]/K_{IPTG}\right)^4} \right) \qquad \textbf{[22]}$$

as quoted in Eq. (3) of the main text for the IPTG response, with $R = 2\,[LacR]/K_1$ and $L_0 = \frac{1}{2}\left([L_{12}]/K_2 + [L_{13}]/K_3\right)$. With DNA looping, the degree of repression becomes

$$f = 1 + R \cdot (L_0 + 1)\,. \qquad \textbf{[23]}$$

From Eq. **22**, it is also straightforward to compute the dependence of sensitivity (defined e.g., as the maximum logarithmic derivative of the transition region) on the loop parameter L_0. We find a monotonic function increasing from ~1.2 for small values of L_0 to ~2.5 at $L_0 = 50$.

[§] In the full thermodynamic treatment, each of the two looping term, $[LacR^{**}][L_{1i}]/K_1K_i$, where $i = 2$ or 3, is further divided by the factor $(1+[LacR^*]/K_i + 2\,[LacR^{**}]/K_i)$. This factor takes into account of the fact that looping of O_1 with the auxiliary operator O_i is not possible if O_i is occupied itself (referred to as the "squelching" effect. We neglected this effect here as the LacR concentration is sufficiently low in wildtype cells. [Note: the squelching term for O1-O3 looping is completely negligible as $2[LacR] \ll K_3$. O1-O2 looping is actually negligible only for $[IPTG] > K_{IPTG}$. This is indeed the regime where most of the data were taken, i.e., most of the data in Fig. 2*a* (squares) are larger than $K_{IPTG} \sim 10\ \mu M$. However, the fact that the data point for [IPTG] = 0 also falls on the same curve (bottom red) suggests that $[L_{12}]/2K_2 \ll [L_{13}]/2K_3$.]

[**] Their values can be indirectly inferred from the experiments of Oehler *et al*. (30) and Muller *et al*. (37) as was done by Vilar and Leibler (40). However the estimates from the two experiments differ by a factor of 5 or more.

In a recent study, Oehler *et al*. (31) characterized the IPTG response for Lac systems incapable of DNA looping (either by the removal of the auxiliary operator O3 or by using mutant LacR incapable of tetramerization) resulted in a noticeable decrease in the cooperativity of the IPTG response of the lac promoter. We analyzed the data published in ref. 31 quantitatively and found those results to match very well with the expected behavior developed in this work: As shown in SI Fig. 7*a*, the IPTG responses for the two systems incapable of DNA looping (red triangles and blue squares) are well-fitted by Eq. **22** with the looping term L_0 set to zero (solid line). The two fitting parameters R ~ 200 and K_{IPTG} ~ 6 μM obtained are consistent with that expected for strains overproducing LacR 5-10x. The ~1000-fold change of the wildtype strain is a consequence of residual affinity of overexpressed LacR for the operator sequences (32); a previous study by Oehler in which the fold change is determined by LacR+/- comparison shows an 8000-fold change as predicted by the model (30).

Combinatorial control by LacR and cAMP-CRP. We now consider the combined control of the *lac* promoter by both LacR and CRP. According to the thermodynamic model, if there is no interaction between CRP-cAMP mediated activation and LacR mediated repression, then the joint dependence would simply be the algebraic product of the activation and repression functions (Eqs. **15** and **20**) in a way analogous to Eq. **14**, i.e.,

$$G = G_0 \cdot \left(\frac{1+\omega\cdot[CRP^*]/K_{CRP}}{1+[CRP^*]/K_{CRP}} \right) \Bigg/ \left(1+\frac{[LacR^*]}{K_1}+\frac{2\,[LacR^{**}]}{K_1}+\frac{[LacR^{**}][L_{12}]}{K_1K_2}+\frac{[LacR^{**}][L_{13}]}{K_1K_3} \right) \quad \textbf{[24]}$$

Alternatively, the co-dependence of the promoter activity on cAMP and IPTG can be obtained from the product of Eq. **16** and Eq. **22**,

$$\alpha = b_0 \cdot \left(\frac{1+\omega\cdot[cAMP]/\kappa_{cAMP}}{1+[cAMP]/\kappa_{cAMP}} \right) \Bigg/ \left(1+\frac{R}{\left(1+[IPTG]/K_{IPTG}\right)^2}+\frac{R\cdot L_0}{\left(1+[IPTG]/K_{IPTG}\right)^4} \right). \quad \textbf{[25]}$$

Note that Eq. **25** is of the same form as the IPTG response of Eq. **22**, but with the basal activity b_0 replaced by α_{cAMP} of Eq. **16**. This corresponds to a simple cAMP-dependent vertical shift of the IPTG response in the log-log plot.

As the data shown in Fig. 2*b* clearly deviated from the above product form (see below), we examined the consequence of a previously proposed interaction between CRP and DNA looping

(18, 33-35). As proposed by Lewis *et al*. (18), upon binding to its operator, CRP induces a 90-130^{o} bend in the DNA, bringing O1 and O3 into closer proximity. This is thought to increase the local concentration $[L_{13}]$, thereby increasing the strength of the looping interaction between them. Experimental evidence for such CRP enhancement of O1-O3 looping has been found *in vitro* (33-35), but no supporting evidence has been reported so far *in vivo*.

This effect can be incorporated into the thermodynamic model developed above simply by including a cooperativity factor $\Omega_0 > 1$ into the term in the denominator of Eq. **24** involving the product of $[CRP^*]$ and $[L_{13}]$. This amounts to changing the factor $[L_{13}]$ appearing in Eq. **24** to

$$[L_{13}] \cdot \left(1 + \Omega_0 \cdot [CRP^*] / K_{CRP}\right) \Big/ \left(1 + [CRP^*] / K_{CRP}\right). \qquad \textbf{[26]}$$

It then follows that the cAMP and IPTG dependence of the promoter activity can be written in the same form as Eq. **25**, but with the looping factor L_0 changed to

$$L = L_0 \cdot \frac{1 + \Omega \cdot [\mathrm{cAMP}] / \kappa_{cAMP}}{1 + [\mathrm{cAMP}] / \kappa_{cAMP}}, \qquad \textbf{[27]}$$

where Ω is an effective cooperativity factor given by

$$\Omega = \left(\frac{[L_{12}]}{K_2} + \Omega_0 \cdot \frac{[L_{13}]}{K_3} \right) \Big/ \left(\frac{[L_{12}]}{K_2} + \frac{[L_{13}]}{K_3} \right). \qquad \textbf{[28]}$$

The parameters $[L_{12}]$, $[L_{13}]$, and Ω_0 have not been determined from direct biochemical studies. However, Fried *et al*. (33, 35) have measured an effective cooperativity factor defined as the ratio of concentration of the cAMP-CRP-LacR-DNA ternary product with the product of the concentrations of cAMP-CRP-DNA and LacR-DNA binary products. In terms of the parameters defined above, this effective cooperativity factor can be written as

$$\frac{\left(1 + \frac{[CRP^*]}{K_{CRP}}\right)\left(1 + R + R \cdot L\right) + \left(\Omega_0 - 1\right) \cdot \frac{[CRP^*]}{K_{CRP}} R \cdot \frac{[L_{13}]}{2K_3}}{\left(1 + \frac{[CRP^*]}{K_{CRP}}\right)\left(1 + R + R \cdot L\right)}. \qquad \textbf{[29]}$$

For saturating amounts of cAMP-CRP and LacR such that $[CRP] \gg K_{CRP}$ and $R \gg 1$, the expression in Eq. **29** is identical to the right hand side of Eq. **28**. Hence, the effective cooperativity factor Ω introduced in Eq. **27** is just the cooperativity factor of the range 4–12 determined experimentally by Fried *et al*. (33, 35).

Finally, we consider the case where $[CRP^*]$ depends nonlinearly on the cAMP concentration of the medium such that the observed cAMP response is described by the general Hill form

$$\alpha_{cAMP} = b_0 \cdot \frac{1 + \omega \cdot \left([cAMP] / C_{cAMP}\right)^m}{1 + \left([cAMP] / C_{cAMP}\right)^m} \qquad \textbf{[30]}$$

with Hill coefficient $m > 1$. This is for example the situation for TK250 cells bearing the *cpdA* gene (see blue symbols in Fig. 1*b*). Working backward from Eq. **15**, we have

$$[CRP^*] = K_{CRP} \left([cAMP] / C_{cAMP}\right)^m \qquad \textbf{[31]}$$

Using Eq. **31** instead of Eq. **8** in the combinatorial control function (Eq. **24** with $[L_{13}]$ replaced by the expression in Eq. **26**, we obtain the following for the co-dependence of the promoter activity:

$$\alpha = b_0 \cdot \left(\frac{1 + \omega \cdot \left([cAMP] / C_{cAMP}\right)^m}{1 + \left([cAMP] / C_{cAMP}\right)^m} \right) \Bigg/ \left(1 + \frac{R}{\left(1 + [IPTG] / K_{IPTG}\right)^2} + \frac{R \cdot L}{\left(1 + [IPTG] / K_{IPTG}\right)^4} \right) \qquad \textbf{[32]}$$

with the loop parameter *L* in Eq. **32** being

$$L = L_0 \cdot \frac{1 + \Omega \cdot \left([\mathrm{cAMP}] / C_{cAMP}\right)^m}{1 + \left([\mathrm{cAMP}] / C_{cAMP}\right)^m}, \qquad \textbf{[33]}$$

and the cooperativity factor Ω in Eq. **33** still given by Eq. **28**.

Comparison to alternative models. While our model described by Eqs. **25** and **27** appears to accurately describe the data (see Fig. 2*b*), one might question whether conceptually simpler models (e.g., generalized Hill functions) might explain the data equally well. Below, we construct several such models and fit to the data surface from strain TK310 using non-linear least squares minimization in Matlab. The points at [IPTG] = 0 are weighted to increase their significance (to simulate the wide range (in log scale) of low IPTG concentrations (< 5 μM) over which the baseline expression from the promoter does not significantly increase). For each model the specified parameters are allowed to vary freely to obtain the optimum fit.

Model a. A naïve 6-parameter model based on generic Hill functions and assuming no interaction between LacR and CRP:

$$\alpha = b_0 \cdot \left(\frac{1+\omega\left([cAMP]/C_{cAMP}\right)^{m_{cAMP}}}{1+\left([cAMP]/C_{cAMP}\right)^{m_{cAMP}}} \right) \Bigg/ \left(1+\frac{R}{1+\left([IPTG]/C_{IPTG}\right)^{m_{IPTG}}} \right) \qquad \textbf{[34]}$$

As can be seen from SI Fig. 8*a*, neither the fold change nor the sensitivity to IPTG response is properly captured by this model for the range of cAMP concentrations studied.

Model b. A 7-parameter model in which the coefficient of the IPTG dependent term, i.e., R in Eq. **34** above, is a four-parameter cAMP-dependent Hill function,

$$R = R_0 \cdot \frac{1+\omega'([cAMP]/C'_{cAMP})^{m_{cAMP}}}{1+([cAMP]/C'_{cAMP})^{m_{cAMP}}}, \qquad \textbf{[35]}$$

where we assume $C'_{cAMP} = C_{cAMP}$, and $m'_{cAMP} = m_{cAMP}$, but allow R_0 and ω' to vary freely. From SI Fig. 8*b*, we see that the fold change of the IPTG response is better reproduced than Model a, but the overall correspondence between data and model prediction is still poor, particularly for intermediate IPTG concentrations (10-500 μM) for both the high and low cAMP levels.

Model c. The same model as Model b, but with C'_{cAMP}, and m'_{cAMP} both varying freely. From SI Fig. 8*c* it is seen that the fit to the data is further improved. However the number of parameters is increased to nine while the fit to data points at intermediate IPTG concentrations is still problematic, especially at low cAMP levels.

Model d. The model Eq. **34** with the modification to R made in Eq. **35**, and with the Hill coefficient m_{IPTG} in Eq. **34** also cAMP dependent. The latter is specified by another Hill function

$$m_{IPTG} = m_0 \cdot \frac{1+\omega''([cAMP]/C''_{cAMP})^{m''_{cAMP}}}{1+([cAMP]/C''_{cAMP})^{m''_{cAMP}}}. \qquad \textbf{[36]}$$

Here, we use $C''_{cAMP} = C'_{cAMP} = C_{cAMP}$, $m''_{cAMP} = m'_{cAMP} = m_{cAMP}$ but allow both ω'' and ω' to vary freely. This 8-parameter model is able to describe the full data set well; see SI Fig. 8*d*. This finding is not surprising given the result in SI Fig. 5*a*, that the effective Hill coefficient of the IPTG response is strongly cAMP dependent.

We see that while both our model (i.e. Eqs. **25** and **27**) and Model d above (i.e., Eqs. **34-36**) adequately describe the experimental data, our model requires seven parameters while Model d requires eight. More importantly, the form used in our model is well founded on known

biochemical facts as described above, and the values of fitted parameters compare favorably with the known range in all cases when comparison can be made. (Note: The loop cost L_0 is the only parameter where independent estimate is not available.) On the other hand, it is difficult to justify biochemically the cAMP-dependence of the Hill coefficient in Model d. The above results therefore demonstrate that our model based on the thermodynamic treatment of DNA looping and its interaction with CRP is the minimal model describing the activity of the *lac* promoter.

Data Analysis. For each strain and medium used, the promoter activity α was computed from the raw data (i.e., β-galactosidase activity and growth curves) according to Eq. **6**. Its dependence on either the concentrations of cAMP or IPTG in the medium was then fitted to an effective Hill form

$$\alpha_X = b_X \cdot \frac{1 + f_X \left([X]/C_X\right)^{m_X}}{1 + \left([X]/C_X\right)^{m_X}} \qquad \textbf{[37]}$$

where $[X]$ refers to the concentration of the inducer X (cAMP or IPTG) in the medium. In the fits, the basal activity b_X was directly fixed by the promoter activity obtained for $[X] = 0$. The other three Hill parameters were obtained by fitting to Eq. **37** using nonlinear least-square minimization (Matlab 7). Reported errors are the 68.3% (1 standard deviation) confidence intervals for the given parameters.

Because DNA looping is involved in repression of the *lac* promoter by the Lac tetramer (17, 29, 30, 36, 37), the IPTG responses of strains TK230 and TK310 (in medium with no cAMP added) were also fitted to the form Eq. **22** predicted by the DNA looping model above. In the fit, we fixed the value of R to 50 as discussed above. We then used the experimentally determined promoter activity in saturating 1 mM IPTG condition to fix the coefficient b_0, and used the remaining data to fit the two parameters K_{IPTG}, and L_0 according the procedure described above. The results are listed in Table 3 (rows 1 and 2). [The values of the IPTG-LacR dissociation constant K_{IPTG} obtained are comparable to the results of *in vitro* biochemical studies: In the absence of DNA, the LacR-IPTG interaction was characterized by K_{IPTG} = 0.8 – 4 μM at physiologically relevant pH values (32, 38, 39). In the presence of a saturating amount of

operator DNA however, a much weaker LacR-IPTG affinity characterized by $K_{IPTG} \approx 80$ μM was found, although with non-specific DNA fragments the smaller value of K_{IPTG} was obtained as before (20). Our results with $K_{IPTG} = 15 \sim 20$ μM lie in between this range, presumably reflecting the interaction of LacR with both specific and non-specific sequences *in vivo*.]

For the IPTG response of strain TK310 and TK250 grown in medium with various cAMP concentrations (the data in Fig. 2*b* and SI Fig. 10*b*), we determined the looping parameter L for the IPTG dependence at each cAMP concentration by first computing the degree of repression f as the ratio of b_0 (determined as above) and the value of the promoter activity at [IPTG] = 0, and then extracting the loop parameter from f using Eq. **23**. The values of L obtained were plotted in Fig. 2*a* and SI Fig. 10*a* for strain TK310 and TK250 respectively. Then for the IPTG response of strain TK310, the predicted form Eq. **25** was plotted as the dashed line in Fig. 2*b* using the values of L shown in Fig. 2*a* and other parameter values as listed in Table 2 (row 2) and Table 3 (row 2). Similarly, for the IPTG response of strain TK250, the predicted form Eq. **32** was plotted as the dashed line in SI Fig. 10*b* using the values of L shown in SI Fig. 10*a* and other parameter values as listed in Table 2 (row 1) and Table 3 (row 3).

Finally, the cAMP dependence of the loop parameter L was analyzed by fitting their values to the expected form according to the extended thermodynamic model, Eq. **27** for strain TK310 and Eq. **33** for strain TK250. In these fits, we varied only the effective cooperativity factor Ω, taking the values of the other parameters from Table 2 (row 2) and Table 3 (row 2) for strain TK310, and Table 2 (row 1) and Table 3 (row 3) for strain TK250. Estimate of error on Ω was again obtained using the procedure described above.

1. Datsenko KA, Wanner BL (2000) *Proc Natl Acad Sci USA* 97: 6640-6645.
2. Simons RW, Houman F, Kleckner, N. (1987) *Gene* 53: 85-96.
3. Miller JH (1972) *Experiments in Molecular Genetics* (Cold Spring Harbor Lab Press, Plainview, NY).
4. Griffith KL, Wolf RE, Jr. (2002) *Biochem Biophys Res Commun* 290: 397-402.
5. Mandelstam J (1957) *Nature* 179: 1179-1181.
6. Wanner BL, Kodaira R, Neidhardt FC (1978) *J Bacteriol* 136: 947-954.
7. Wanner BL, Kodaira R, Neidhardt FC (1977) *J Bacteriol* 130: 212-222.
8. Malan TP, Kolb A, Buc H, McClure WR (1984) *J Mol Biol* 180: 881-909.
9. Takahashi M, Blazy B, Baudras A (1980) *Biochemistry* 19: 5124-5130.

10. Takahashi M, Blazy B, Baudras A, Hillen W (1989) *J Mol Biol* 207: 783-796.
11. Fried MG, Crothers DM (1984) *J Mol Biol* 172: 241-262.
12. Garner MM, Revzin A (1982) *Biochemistry* 21: 6032-6036.
13. Brown AM, Crothers DM (1989) *Proc Natl Acad Sci USA* 86: 7387-7391.
14. Saier MH, Jr, Feucht BU, McCaman MT (1975) *J Biol Chem* 250**:** 7593-7601.
15. Goldenbaum PE, Hall GA (1979) *J Bacteriol* 140: 459-467.
16. Epstein W, Rothman-Denes LB, Hesse J (1975) *Proc Natl Acad Sci USA* **72:** 2300-2304.
17. Muller-Hill B (1996) *The lac Operon* (de Gruyter, Berlin).
18. Lewis M, Chang G, Horton NC, Kercher MA, Pace HC, Schumacher MA, Brennan RG, Lu P (1996) *Science* 271: 1247-1254.
19. Winter RB, Berg OG, von Hippel PH (1981) *Biochemistry* 20: 6961-6977.
20. O'Gorman RB, Rosenberg JM, Kallai OB, Dickerson RE, Itakura K, Riggs AD, Matthews KS (1980) *J Biol Chem* 255: 10107-10114.
21. Ackers GK, Johnson AD, Shea MA (1982) *Proc Natl Acad Sci USA* 79: 1129-1133.
22. Buchler NE, Gerland U, Hwa T (2003) *Proc Natl Acad Sci USA* 100: 5136-5141.
23. Bintu L, Buchler NE, Garcia HG, Gerland U, Hwa T, Kondev J, Kuhlman T, Phillips R (2005) *Curr Opin Genet Dev* 15: 125-135.
24. Bintu L, Buchler NE, Garcia HG, Gerland U, Hwa T, Kondev J, Phillips R (2005) *Curr Opin Genet Dev* 15: 116-124.
25. Gerland U, Moroz JD, Hwa, T. (2002) *Proc Natl Acad Sci USA* 99: 12015-12020.
26. Cossart P, Gicquel-Sanzey B (1985) *J Bacteriol* 161: 454-457.
27. Schmitz A, Galas DJ (1979) *Nucleic Acids Res* 6: 111-137.
28. Gilbert W, Gralla JD, Majors J, Maxam A (1975) in *Protein-Ligand Interactions*, eds Sund H, Blauer R (de Gruyter, Berlin-New York), pp. 193-206.
29. Oehler S, Eismann ER, Kramer H, Muller-Hill B (1990) *EMBO* **9:** 973-979.
30. Oehler S, Amouyal M, Kokhof P, von Wilcken-Bergmann B, Muller-Hill B (1994) *EMBO* **13:** 973-979.
31. Oehler S, Alberti S, Muller-Hill B (2006) *Nucleic Acids Res* 34: 606-612.
32. Gilbert W, Muller-Hill B (1970) in *The Lactose Operon*, eds Beckwith, J. & Zipser, D. (Cold Spring Harbor Lab Press, Plainview, NY), pp. 93-109.
33. Fried MG, Hudson JM (1996) *Science* 274: 1930-1, and author reply (1996) 274: 1931-1932.
34. Hudson JM, Fried MG (1990) *J Mol Biol* 214: 381-396.
35. Vossen KM, Stickle DF, Fried MG (1996) *J Mol Biol* 255: 44-54.
36. Eismann ER, Muller-Hill B (1990) *J Mol Biol* 213: 763-775.
37. Muller J, Oehler S, Muller-Hill B (1996) *J Mol Biol* 257: 21-29.
38. Nichols JC, Matthews KS (1997) *J Biol Chem* 272: 18550-18557.
39. Jobe A, Bourgeois S (1972) *J Mol Biol* 69: 397-408.
40. Vilar JM, Leibler S (2003) *J Mol Biol* 331: 981-989

Table 4: List of strains and plasmids used in this study.

1. Datsenko KA, Wanner BL (2000) *Proc Natl Acad Sci USA* 97: 6640-6645.

Strain	Genotype	Derived From	Comments
TK110	Δ*cpdA*	MG1655	deletion from 3174100 to 3174793
TK120	Δ*crp*	MG1655	deletion from 3483856 to 3484369
TK130	Δ*cyaA*	MG1655	deletion from 3988871 to 3991173
TK140	Δ*lacI*	MG1655	deletion from 365748 to 366642
TK150	Δ*lacY*	MG1655	deletion from 361259 to 362274
TK200	Δ*lacI ΔlacY*	TK140	
TK210	Δ*cpdA ΔlacY*	TK110, TK150	
TK220	Δ*crp ΔlacI*	TK110, TK140	
TK230	Δ*crp ΔlacY*	TK120, TK150	
TK240	Δ*cyaA ΔlacI*	TK130, TK140	
TK250	Δ*cyaA ΔlacY*	TK130, TK150	
TK310	Δ*cyaA ΔcpdA ΔlacY*	TK110, TK130, TK150	
TK320	Δ*cyaA ΔlacI ΔlacY*	TK130, TK200	
TK330	Δ*crp ΔlacI ΔlacY*	TK120, TK200	
BW25113	$lacI^q$ $rrnB_{T14}$ Δ$lacZ_{WJ16}$ *hsdR514* Δ$araBAD_{AH33}$ Δ$rhaBAD_{LD78}$	K12 BD792	ref. 1
TK400	Δ*cyaA*	BW25113	deletion from 3988871 to 3991173
TK500	Δ*cyaA* Φ(P*crp-lacZ*)	TK400	P*crp* amplified from 3483424 to 3483721
TK600	Δ*cyaA* Φ(P*lac*Δ*crp-lacZ*)	TK400	CRP operator at -61.5 altered from TGTGAGTTAGCTCACT to CAGACGTTAGCTCACT

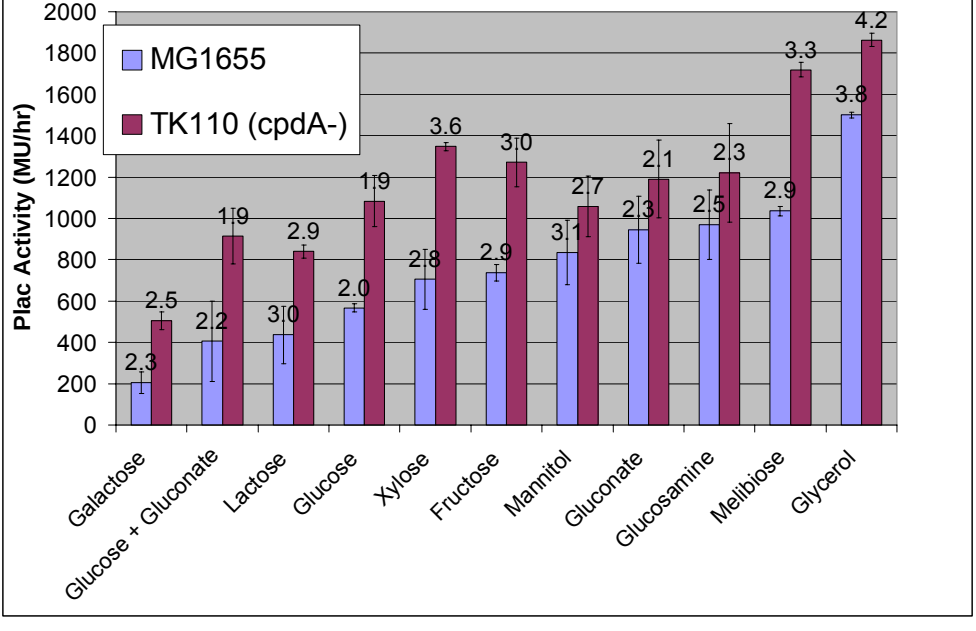
MG1655
TK110 (cpdA-)
Plac Activity (MU/hr)
2000
1800
1600
1400
1200
1000
800
600
400
200
0
2.3
2.5
2.2
1.9
3.0
2.9
2.0
1.9
2.8
3.6
2.9
3.0
3.1
2.7
2.3
2.1
2.5
2.3
2.9
3.3
3.8
4.2
Galactose
Glucose + Gluconate
Lactose
Glucose
Xylose
Fructose
Mannitol
Gluconate
Glucosamine
Melibiose
Glycerol

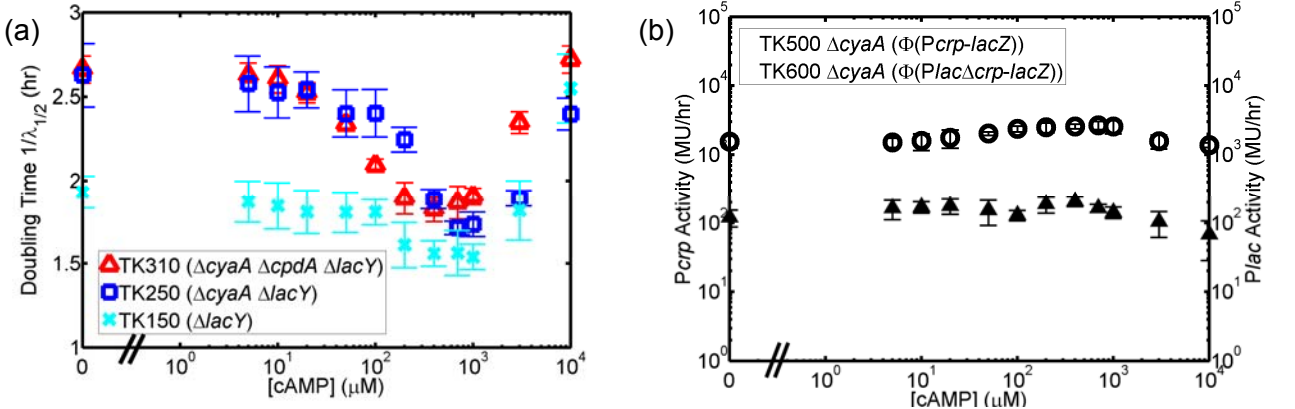
(a)
Doubling Time $1/\lambda_{1/2}$ (hr)
[cAMP] (μM)
TK310 (ΔcyaA ΔcpdA ΔlacY)
TK250 (ΔcyaA ΔlacY)
TK150 (ΔlacY)
(b)
TK500 ΔcyaA (Φ(Pcrp-lacZ))
TK600 ΔcyaA (Φ(PlacΔcrp-lacZ))
Pcrp Activity (MU/hr)
Plac Activity (MU/hr)
[cAMP] (μM)

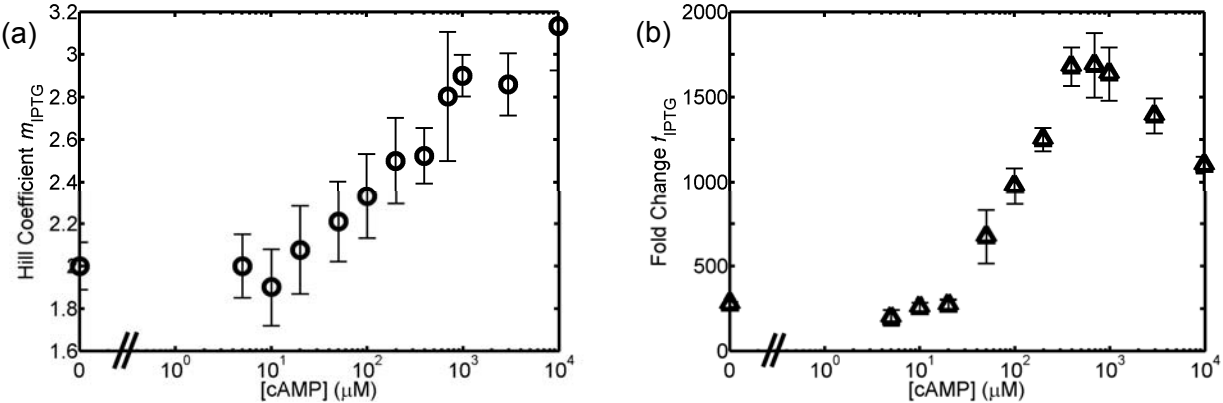
(a)
Hill Coefficient m_{IPTG}
3.2
3
2.8
2.6
2.4
2.2
2
1.8
1.6
0
10^0
10^1
10^2
10^3
10^4
[cAMP] (μM)
(b)
Fold Change f_{IPTG}
2000
1500
1000
500
0
10^0
10^1
10^2
10^3
10^4
[cAMP] (μM)

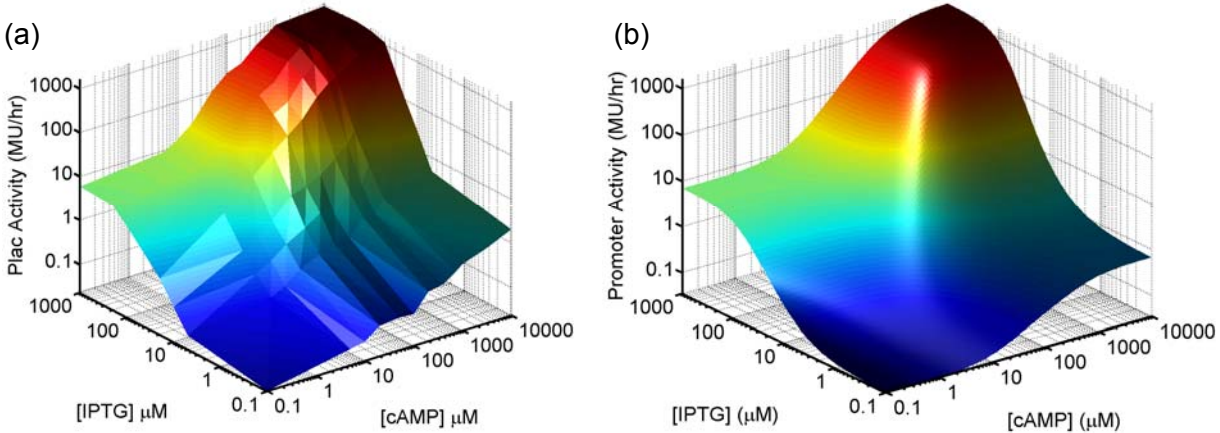
(a)
Plac Activity (MU/hr)
1000
100
10
1
0.1
1000
100
10
1
0.1
[IPTG] μM
0.1
1
10
100
1000
10000
[cAMP] μM
(b)
Promoter Activity (MU/hr)
1000
100
10
1
0.1
1000
100
10
1
0.1
[IPTG] (μM)
0.1
1
10
100
1000
10000
[cAMP] (μM)

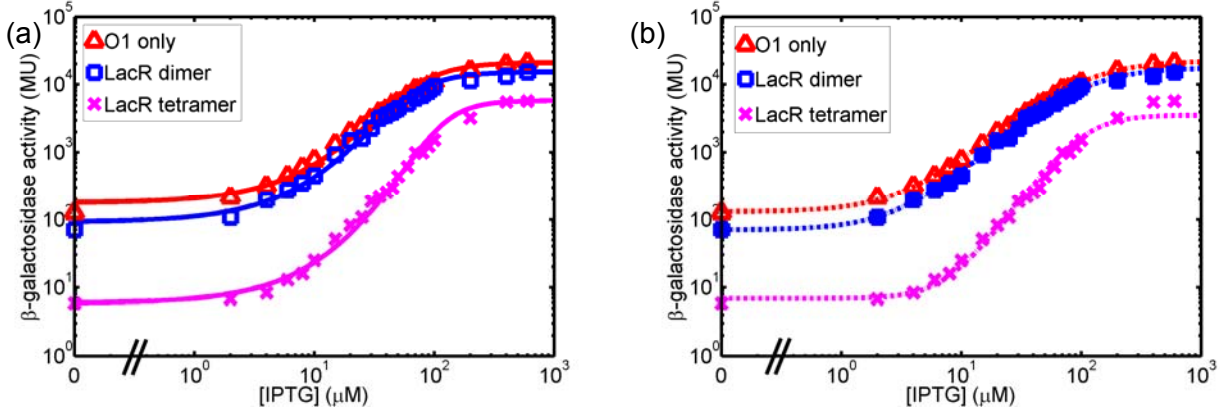
(a)
O1 only
LacR dimer
LacR tetramer
β-galactosidase activity (MU)
[IPTG] (μM)
(b)
O1 only
LacR dimer
LacR tetramer
β-galactosidase activity (MU)
[IPTG] (μM)

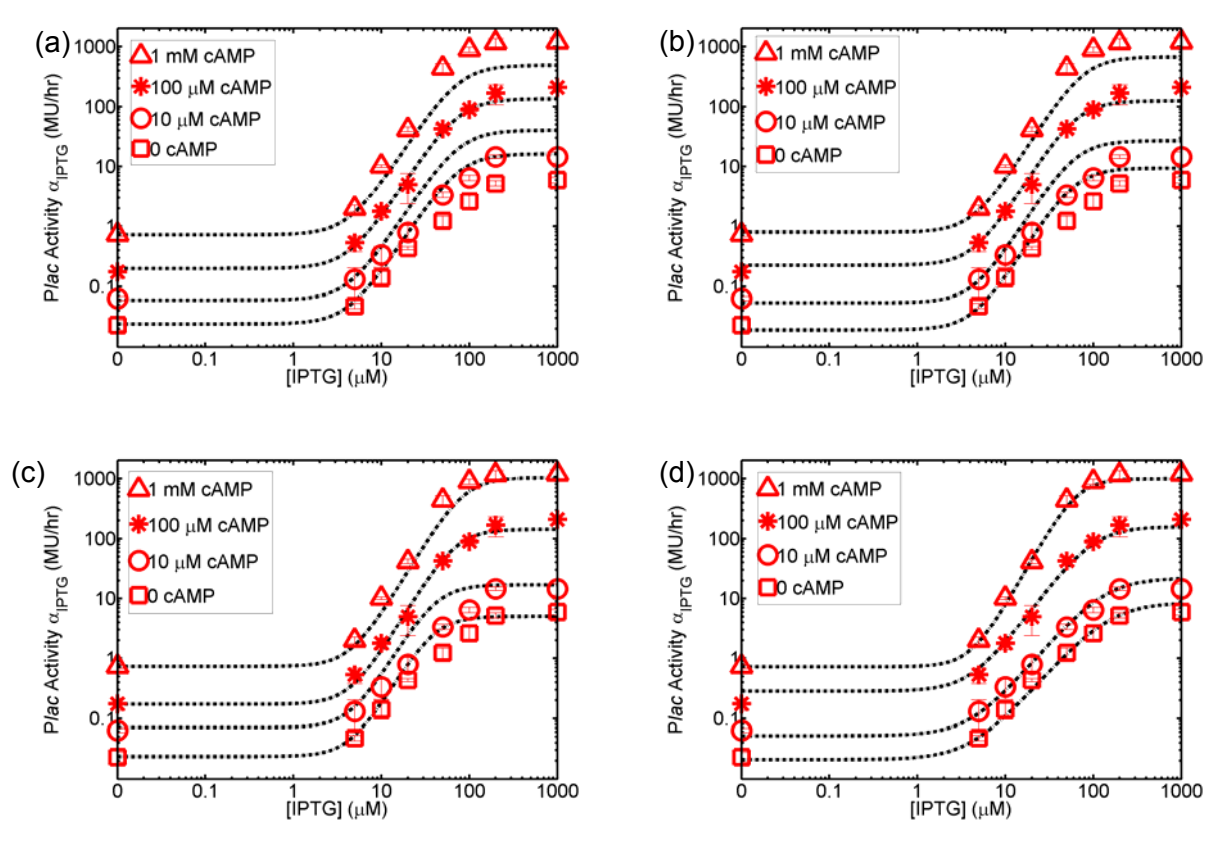
(a)
(b)
(c)
(d)
1 mM cAMP
100 μM cAMP
10 μM cAMP
0 cAMP
P/ac Activity α_IPTG (MU/hr)
[IPTG] (μM)
0
0.1
1
10
100
1000

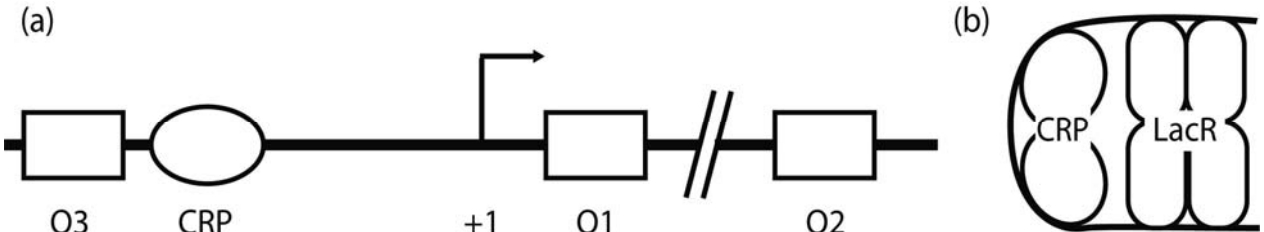
(a)
O3
CRP
+1
O1
O2
(b)
CRP
LacR

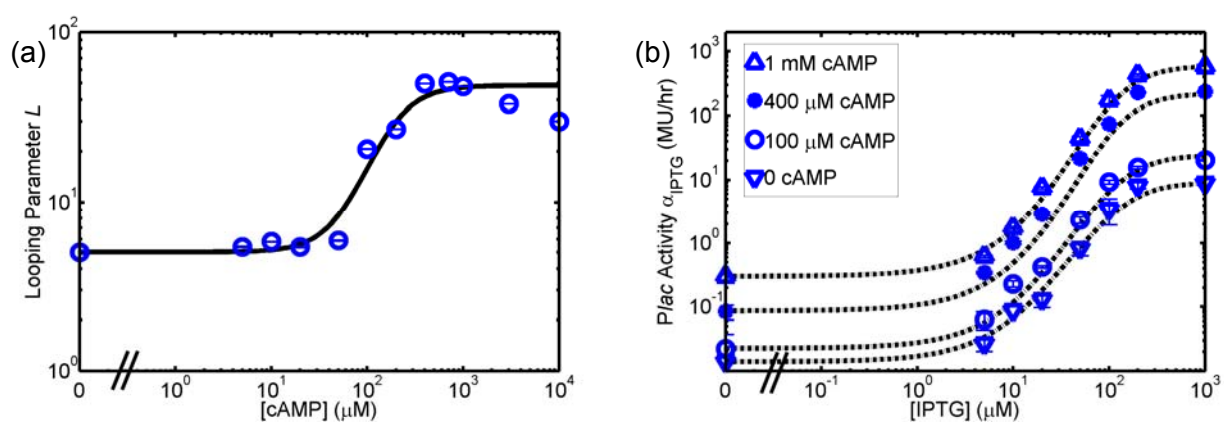
(a)
Looping Parameter L
[cAMP] (μM)
(b)
1 mM cAMP
400 μM cAMP
100 μM cAMP
0 cAMP
Plac Activity αIPTG (MU/hr)
[IPTG] (μM)